

Description of rock samples from a West Greenland drillcore

Henriette Hansen



GEOLOGICAL SURVEY OF DENMARK AND GREENLAND
MINISTRY OF THE ENVIRONMENT



Description of rock samples from a West Greenland drillcore

Henriette Hansen

Released 31.12.2005

Description of rock samples from a West Greenland drillcore

Henriette Hansen

Geological Survey of Denmark and Greenland
Øster Voldgade 10
DK-1350 Copenhagen K

Contents

Summary	3
Objective	3
Petrography.....	4
Mineral chemistry	10
Chemical composition.....	13
Classification	15
Conclusions.....	16
References.....	17
Appendix 1	18

Summary

Rock samples from a drillcore in West Greenland are described and analysed for mineral compositions by use of electron microprobe. Whole rock compositions are furthermore determined through X-ray fluorescence analysis.

The rock is phlogopite-ilmenite-magnetite-clinopyroxene macrocrystic with a groundmass consisting mainly of carbonate, titanomagnetite and phlogopite. Olivine is likely to have been present in the rock, but is now altered to mainly carbonates and some amphibole. It is best classified as an ultramafic lamprophyre, possibly an aillikite.

Objective

The purpose of this report is to describe selected rock samples of a drillcore for the Bureau of Minerals and Petroleum in i Nuuk, Greenland.

Petrography

Macroscopic description

The supplied drillcore samples are of a light grey, inequigranular igneous rock with numerous dark micaceous macrocrysts in a carbonate-rich matrix. Some 1mm-2 cm white, red-violet, green and pale yellow-brown irregularly shaped inclusions have white (red-violet inclusions) or dark (white and yellow-brown inclusions) coloured alteration rims indicating disequilibrium with the host material. The drillcore is cut by 1-2 mm thick white carbonate veins with dark rims.

Microscopic descriptions

Phlogopite-ilmenite-clinopyroxene macrocrystic igneous rock with a groundmass of mainly carbonate (≥ 50 vol. % of the groundmass), titanomagnetite (5-10 vol. % of the groundmass) and phlogopite. Chalcopyrite (0.01-0.03 mm) is disseminated in the rock. No olivine has been identified, but some completely altered phases may originally have been olivine.

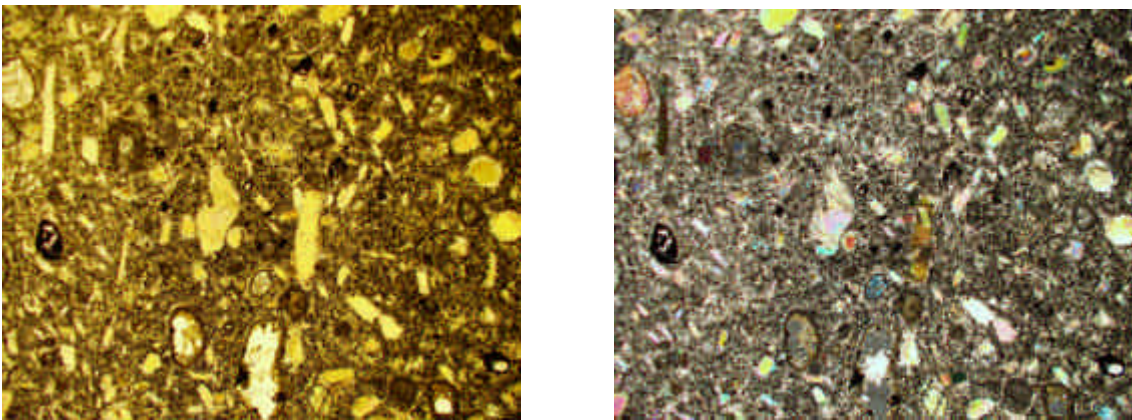


Fig. 1: *Phlogopite macrocrysts, the longest dimension of largest crystals is approximately 1.5 mm. In the left photo light is planepolarized, in the right photo polars are crossed. Deformation structures are visible in the two large mica phenocrysts in the middle of the photographs.*

Phlogopite macrocrysts are 0.5-4 mm large, elongate subhedral or anhedral platy crystals with distinct pleochroism from colourless to light brown to green. The abundance of phlogopite macrocrysts is estimated to 5-7 vol. %. The lightest pleochroitic colour is present when mineral cleavage is oriented E-W on the microscope stage. Some crystals are deformed and partially recrystallised (Fig. 1, 2), and many have a concentric rim zone with a different composition (Fig. 3). Phlogopite is also occasionally found intergrown with ilmenite (Fig. 4).

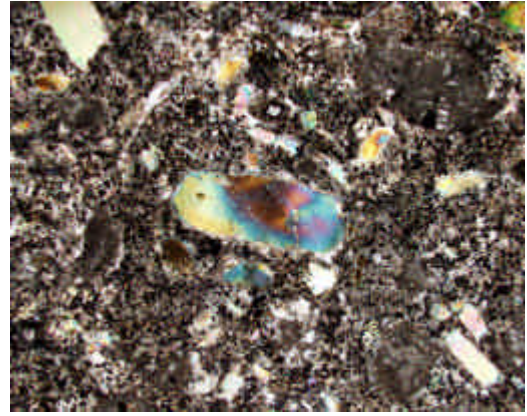
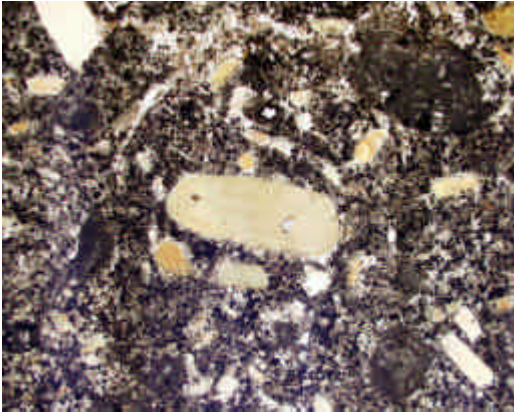


Fig. 2: Deformed phlogopite macrocryst in center of view. In the left photo light is planepolarized, in the right photo polars are partially crossed to expose the deformation patterns. The deformed crystal is 1.38 mm in the longest dimension.

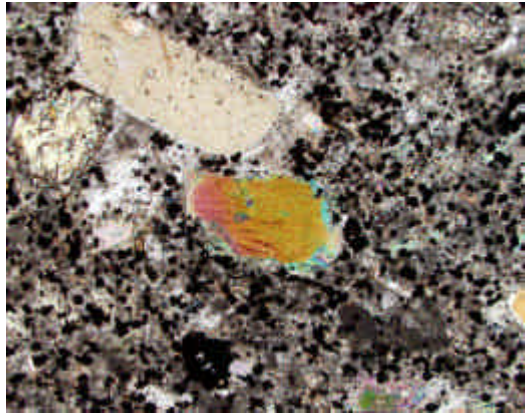
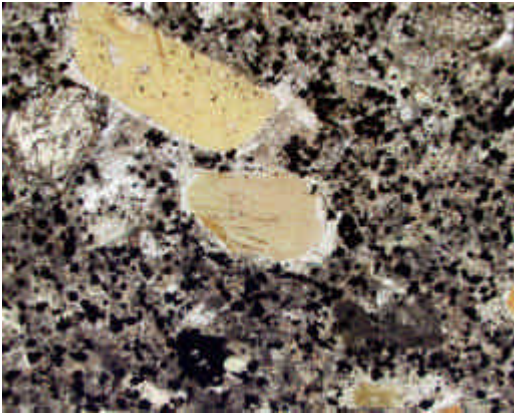


Fig. 3: Two zoned phlogopite macrocrysts. In the left photo light is planepolarized, in the right photo polars are crossed. The phlogopite nearest the center of view is 0.85 mm in the longest dimension.

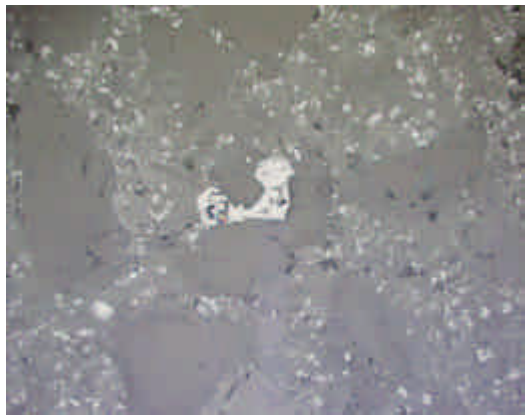
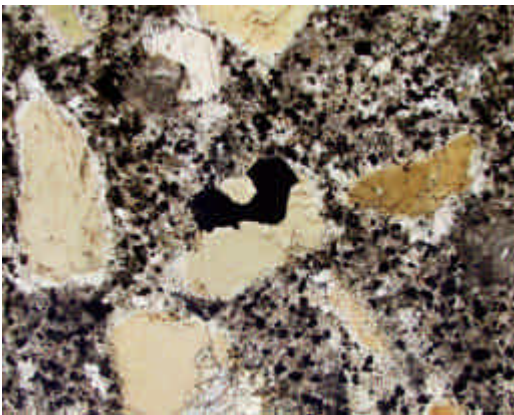


Fig. 4: Intergrown phlogopite (brown in left photo, dark grey in right photo) and ilmenite (black in left photo, light grey in right photo) in center of view. The phlogopite macrocrysts have thin rim zones. In the left photo light is planepolarized and transmitted, the right photo is taken in reflected light. The longest dimension of the phlogite macrocryst near the left edge of the photographs is 0.63 mm.

Ilmenite macrocrysts are subhedral to anhedral, commonly with rounded shapes (Fig. 5). They are 0.5-3 mm large, make up 2 to 3 vol. % of the rock, and some ilmenite microcrysts have titanomagnetite rims (Fig. 6).

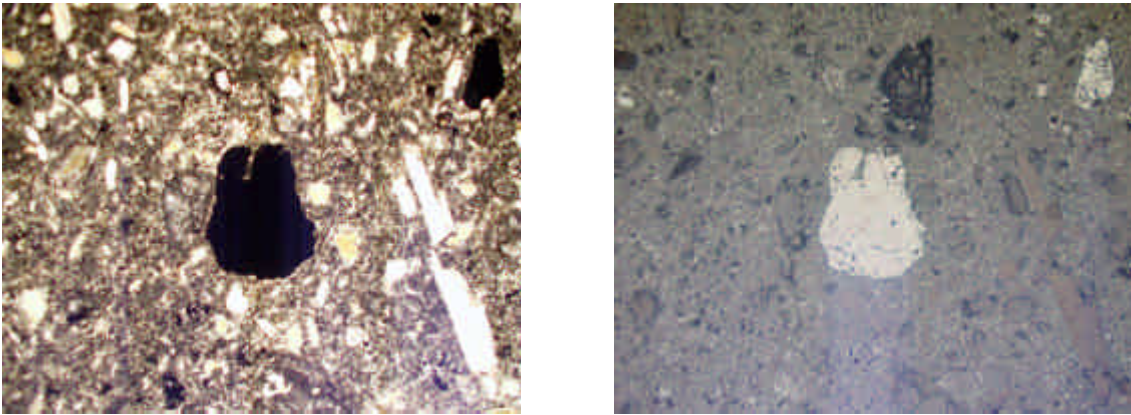


Fig. 5: *Ilmenite macrocryst (black in left photo, light grey in right photo) in center of view and in upper right corner. The longest dimension of the ilmenite is c. 2.4 mm. In the left photo light is transmitted planepolarized, the right photo is taken in reflected light.*

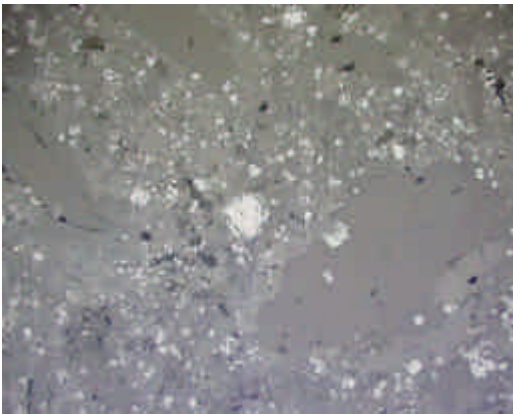


Fig. 6: *Ilmenite microcryst (light, reddish grey, c. 0.3 mm in diameter) mantled by titanomagnetite (light grey) in center of view. The light grey skeletal groundmass minerals are titanomagnetite. Photo taken in reflected light.*

Clinopyroxene macrocrysts are light green, anhedral and often spongy (Fig. 7, 8), which is indicative of disequilibrium with the groundmass. They form less than 1 vol. % of the rock, and are 0.5-1.3 mm. Some clinopyroxene enclose euhedral phlogopite crystals (Fig. 8), possibly as a result of reaction between the clinopyroxene and the host rock.

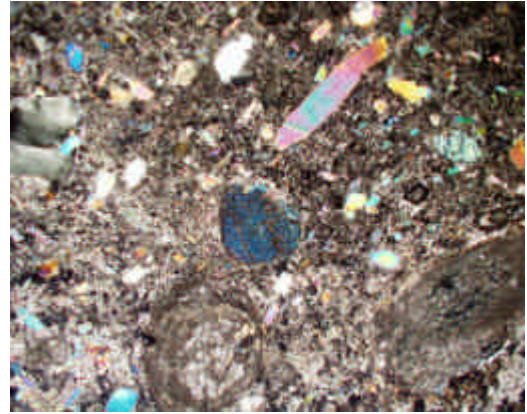
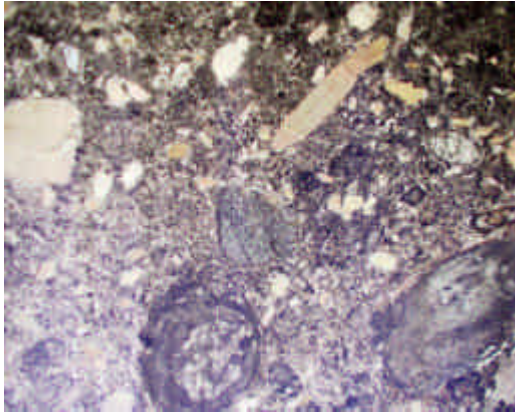


Fig. 7: Anhedra rounded and spongy clinopyroxene macrocryst in center of photographs. The clinopyroxene is green in the transmitted planepolarized light of the left photo, and blue in the right photo where nicols are crossed. The largest dimension of the clinopyroxene is 1.5 mm. A rounded carbonate inclusion is present just below the clinopyroxene.

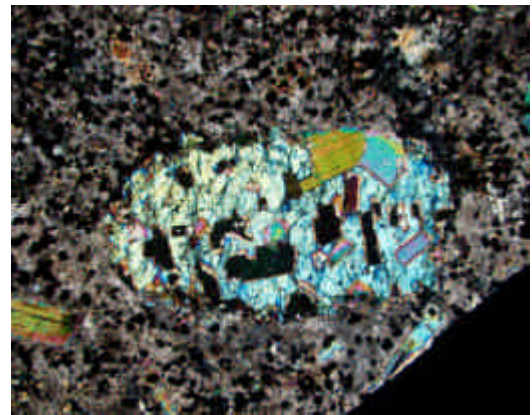
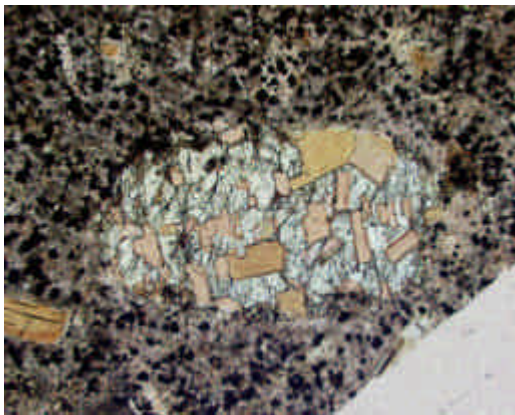


Fig. 8: Anhedra clinopyroxene macrocryst (green in left photo) with embedded euhedral phlogopite (light brown in left photo). The longest dimension of the clinopyroxene is 1.1 mm. The left photo is taken in transmitted planepolarized light, in the photo to the right polars are crossed.

In the groundmass, much of the titanomagnetite is skeletal (Fig. 6), suggesting rapid crystallisation of the oxide. The carbonate is micro- to cryptocrystalline and along with titanomagnetite it is partially included in groundmass micas (probably phlogopite).

Rounded, polycrystalline white and yellowish inclusions of carbonate (Fig. 7, 9) ranging in size from about one mm to about one cm have concentric fractures in the rim region. There are dark cryptocrystalline reaction zones around the inclusions. Sometimes the carbonate inclusions contain one or more colourfree minerals with lower birefringence than the carbonate. These minerals may be scapolite or cancrinite.

There are two types of red-violet inclusions (Fig. 10, 11). One type consist mainly of carbonate, another has some quartz and feldspar in addition to the carbonate and are probably derived from a gneiss or granite. Both inclusion types are intensely fractured and (in transmitted light) black along the fractures, most likely as a result of oxidation. The reaction rims around the inclusions consist of cryptocrystalline material.

Green inclusions consist of green cryptocrystalline material and some euhedral phlogopites.

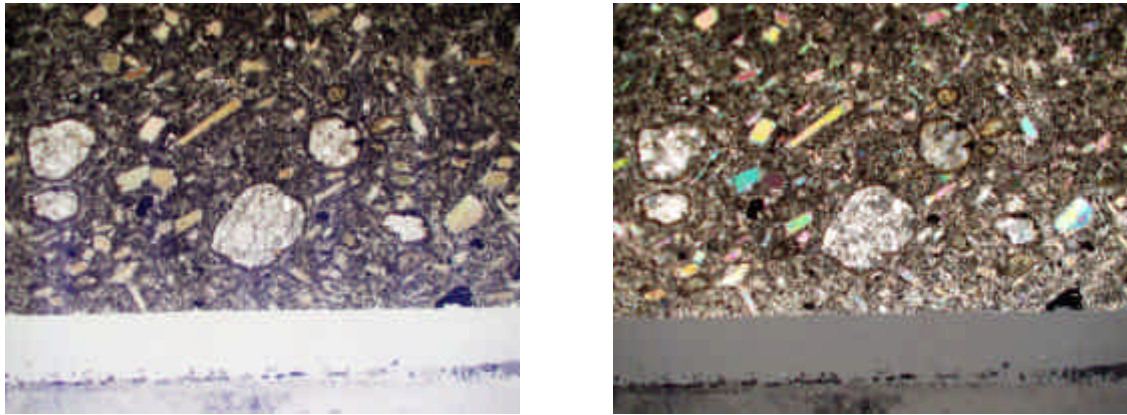


Fig. 9: *Rounded carbonate inclusions with dark cryptocrystalline reaction rims. The left photo is in plane-polarised light, the right is with polars crossed. The largest dimension of the largest inclusion is 1.5 mm.*

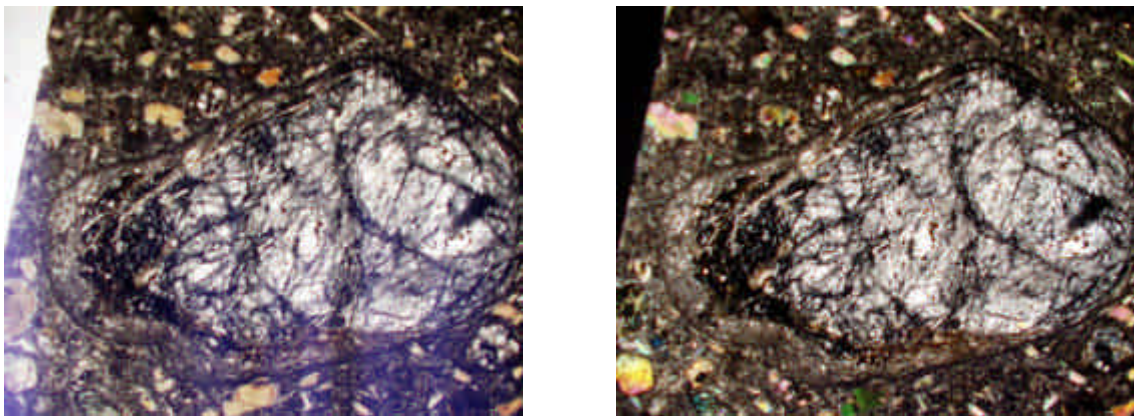


Fig. 10: *Rounded carbonate inclusion with cryptocrystalline reaction rim. This inclusion appears red-violet in hand specimen of the drillcore. The left photo is in plane-polarised light, the right is with polars crossed. The inclusion is 7 mm wide and 4 mm across.*

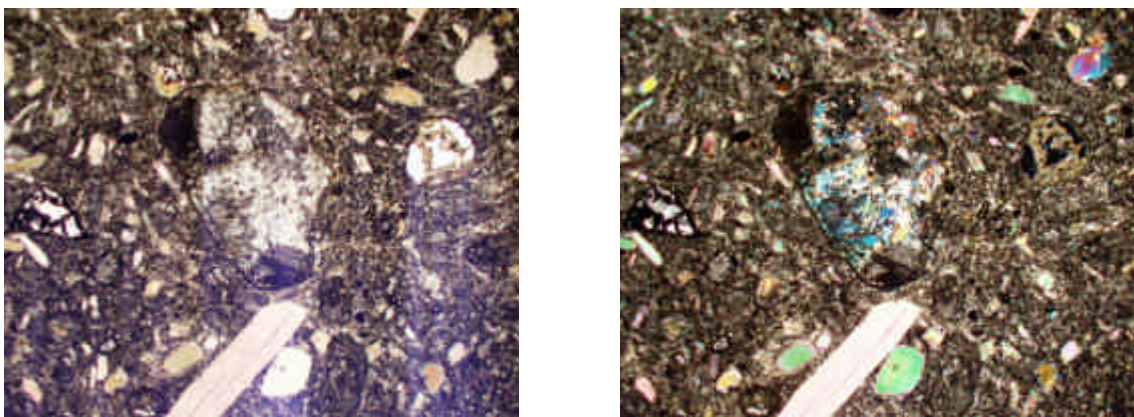


Fig. 12: *Red-violet, c. 5 mm inclusion (center of view) with feldspar and quartz in addition to carbonate. The left photo is in plane-polarised light, the right is with polars crossed.*

Carbonate veins (Fig. 12) contain intergranular carbonate ranging in size from c. 0.025 mm to 0.38 mm, and the dark edges are cryptocrystalline. There is no preferred orientation of vein minerals.



Fig. 12: Carbonate vein photographed in transmitted light with polars crossed. The vein width is 1 mm.

Mineral chemistry

Macrocrysts and some matrix minerals were chemically analysed using the Jeol Superprobe at the Geological Institute, University of Copenhagen. Acceleration voltage was 15 kV, electron beam current 15 nA and the diameter of the beam was set to 5 μm in order to minimize volatilisation of the light elements mainly hosted in phlogopite. Standards were a mixture of pure elements and minerals, and the analyses were made using wavelength dispersive spectra only. Each grain analysis is the average of three to five point analyses, and data are listed in Table 1. The position of individual analyses are shown in the electron backscatter images in Appendix 1. Most minerals are concentrically zoned, but some zoning patterns are slightly more complex as shown by, e.g., the clinopyroxene in Image 160 of Appendix 1.

Clinopyroxene has MgO in the range 14-17 wt. %, CaO 17-25 wt. %, and Al_2O_3 0.6-2.3 wt. %. Cr_2O_3 contents are low (0-0.6 wt. %). All rim analyses are richer in MgO than the corresponding cores, and there is also a tendency for Al_2O_3 and TiO_2 to be more enriched in the rim regions. The SiO_2 content is lower in clinopyroxene rims than in cores.

Phlogopite has 9-10 wt. % K_2O , 18-24 wt. % MgO, 10-17 wt. % Al_2O_3 and 0.7-3.9 wt. % TiO_2 . Cl contents are negligible, whereas some F is present, 0.3-0.8 wt. %. Rims of macrocrysts are richer in Al_2O_3 , MgO, K_2O and F than the cores, and also contain less SiO_2 , FeO and Na_2O than the core regions.

Ilmenite is MgO-rich (8-10 wt. %), and occasionally rich in Cr_2O_3 (0-4.8 wt. %). It is found as macrocrysts, inclusions (A9-2 in Table 1, Image 142 of Appendix 1) in clinopyroxene, and as inclusions (A14-1 in Table 1, Image 147 of Appendix 1) in possible remnants after olivine (A14-2 in Table 1, Image 147).

Cr-rich spinel has Cr_2O_3 about 37 wt. %, 9 wt. % MgO, 5 wt. % Al_2O_3 and 8 wt. % TiO_2 . The Cr-rich spinel was enclosed in alteration minerals that probably replaced olivine phenocrysts (A16-3 in Table 1).

Olivine has not been identified, but Mg-rich carbonate (A14-2 in Table 1) could have replaced olivine. Analysis A16-3C (Table 1, Image 154) is close to a magnesioriebeckite composition. This amphibole has been identified in the Sarfartoq carbonatite complex where it replaces olivine (Secher & Larsen, 1980; Larsen & Secher, pers. comm.). The presence of Cr-rich spinel in close association with the magnesioriebeckite supports that olivine could have been a macrocryst phase in the rock. The similar zoning patterns in phlogopite and clinopyroxene for SiO_2 , Al_2O_3 and MgO suggests that SiO_2 is removed during silicate crystallisation, whereas Al_2O_3 and MgO increase. The increase in MgO may be caused by the tendency of its main competitor in the silicate structure, Fe, to form oxides in the form of ilmenite and magnetite. Although Al_2O_3 form a significant part of the phlogopite structure, phlogopite crystallisation has not been capable of depleting the melt in Al. This may be due the large input of Al-rich crustal xenoliths (gneiss, sediments) late in the crystallisation history of the rock.

Grain	SiO ₂	TiO ₂	Al ₂ O ₃	FeO	MnO	MgO	CaO	Na ₂ O	K ₂ O	Cr ₂ O ₃	NiO	Cl	F	SUM
A1-1	54.11	0.13	0.70	6.97	0.19	15.12	22.44	1.17	0.02	0.02	0.04	0.01	0.01	100.93
A1-1	55.08	0.13	0.65	5.54	0.18	15.72	23.55	0.78	0.01	0.01	0.02	0.01	0.00	101.67
A3-1	54.08	0.64	0.99	6.15	0.18	15.85	22.51	0.88	0.00	0.04	0.04	0.01	0.02	101.37
A3-1	53.65	0.59	0.96	6.69	0.14	15.57	22.60	0.84	0.01	0.01	0.01	0.00	0.01	101.09
A3-1	52.39	0.76	2.27	6.65	0.14	17.27	16.95	1.25	1.71	0.00	0.01	0.01	0.48	99.89
A4-1	54.45	0.12	0.97	7.68	0.18	14.63	21.87	1.44	0.00	0.00	0.00	0.00	0.01	101.36
A4-1	53.26	0.49	1.36	5.11	0.18	15.30	24.63	0.64	0.02	0.00	0.02	0.00	0.00	101.02
A9-1	54.60	0.22	0.58	6.16	0.13	16.35	21.86	0.96	0.02	0.05	0.02	0.01	0.01	100.95
A14-3	54.40	0.21	0.54	6.00	0.15	16.13	21.84	0.97	0.01	0.05	0.02	0.01	0.00	100.33
A17-2	54.43	0.21	1.59	8.56	0.17	14.08	20.52	1.71	0.02	0.15	0.01	0.00	0.01	101.46
A18-1	54.08	0.12	1.96	7.34	0.18	14.04	21.04	1.87	0.01	0.56	0.01	0.00	0.02	101.24
A21-2	53.93	0.13	1.01	7.86	0.17	14.21	21.97	1.42	0.01	0.01	0.02	0.00	0.00	100.73
A2-1	40.53	1.47	11.94	8.88	0.05	21.88	0.09	0.66	9.20	0.03	0.02	0.03	0.45	95.23
A2-1	36.62	1.53	16.09	5.28	0.04	22.35	0.27	0.38	8.90	0.03	0.02	0.03	0.56	92.10
A2-2	37.95	2.02	15.84	11.56	0.12	17.96	0.00	0.86	9.31	0.04	0.05	0.01	0.30	96.01
A2-2	37.96	2.93	14.56	8.24	0.04	20.12	0.67	0.83	9.16	0.04	0.05	0.02	0.34	94.94
A2-2	35.87	1.29	17.32	4.13	0.02	22.60	0.01	0.31	9.24	0.05	0.01	0.01	0.67	91.54
A4-2	40.21	1.06	12.85	9.69	0.05	21.67	0.11	1.10	9.05	0.05	0.05	0.01	0.42	96.32
A6-1	39.44	3.86	13.66	6.65	0.00	20.90	0.08	0.57	9.76	0.82	0.13	0.02	0.26	96.16
A6-1	39.31	3.88	13.62	6.62	0.02	20.84	0.12	0.53	9.56	0.83	0.12	0.05	0.30	95.79
A8-1	41.80	0.76	10.31	9.38	0.03	23.05	0.01	0.67	9.58	0.06	0.00	0.01	0.66	96.31
A10-1	40.65	0.90	12.06	9.02	0.07	22.40	0.00	0.73	9.42	0.00	0.01	0.01	0.52	95.79
A14-4	41.10	1.16	11.85	8.34	0.03	22.69	0.00	0.86	9.37	0.03	0.02	0.01	0.50	95.97
A14-6	40.61	0.71	12.04	8.42	0.04	23.13	0.00	0.78	9.51	0.03	0.00	0.01	0.59	95.88
A17-1	39.72	1.42	13.22	11.09	0.05	20.38	0.02	0.94	8.99	0.05	0.05	0.02	0.43	96.39
A17-1	37.29	1.06	16.83	3.91	0.04	23.90	0.04	0.26	9.88	0.03	0.04	0.01	0.78	94.08
A19-1	38.48	1.23	15.52	4.64	0.07	24.03	0.03	0.26	10.07	0.01	0.00	0.01	0.84	95.20
A23-1	40.63	1.44	12.27	9.24	0.05	21.95	0.00	0.71	9.46	0.03	0.00	0.01	0.48	96.26
A23-1	38.59	1.24	15.43	4.91	0.08	24.08	0.05	0.24	10.25	0.02	0.02	0.01	0.76	95.66
A25-1	40.24	3.66	12.82	6.95	0.03	21.47	0.01	0.57	9.85	0.25	0.09	0.01	0.41	96.36
A3-2	7.70	6.77	0.90	42.03	0.13	8.70	12.68	0.30	0.17	0.29	0.06	0.02	0.04	79.80
A5-1	0.24	5.57	1.19	85.99	0.24	2.02	0.00	0.01	0.00	0.06	0.00	0.00	0.00	95.34
A5-1	0.10	5.39	1.19	85.05	0.36	2.20	0.71	0.01	0.00	0.04	0.01	0.00	0.00	95.06
A7-2	4.10	2.82	0.38	74.35	0.13	1.82	1.96	0.10	0.08	1.65	0.09	0.02	0.00	87.51
A11-1	0.24	31.61	0.27	25.30	0.27	11.18	11.92	0.03	0.03	2.92	0.10	0.00	0.01	83.87
A12-1	1.96	3.50	0.15	81.16	0.06	0.09	0.60	0.14	0.01	0.30	0.03	0.02	0.00	88.01
A13-1	0.45	4.40	0.44	87.11	0.09	0.31	0.05	0.03	0.00	0.07	0.00	0.00	0.00	92.95
A13-1	1.01	4.59	0.78	82.70	0.18	1.47	1.42	0.03	0.07	0.17	0.03	0.00	0.00	92.47
A14-5	0.08	6.12	0.88	84.60	0.22	2.25	0.01	0.02	0.00	0.60	0.00	0.00	0.00	94.78
A15-1	0.34	6.15	0.99	82.95	0.37	3.11	0.01	0.03	0.00	0.05	0.00	0.01	0.00	94.01
A15-1	0.09	6.25	0.95	83.97	0.33	2.22	0.02	0.05	0.01	0.06	0.01	0.01	0.00	93.97
A15-2	0.95	2.11	0.28	87.61	0.03	0.09	0.12	0.04	0.00	0.04	0.03	0.01	0.00	91.29
A15-3	0.12	7.41	0.64	82.66	0.32	3.24	0.06	0.02	0.00	0.09	0.01	0.00	0.00	94.57
A21-1	1.07	1.44	0.11	88.46	0.03	0.09	0.11	0.07	0.01	0.25	0.04	0.02	0.00	91.71
A20-1	0.90	4.91	0.19	84.42	0.37	0.96	0.34	0.07	0.01	0.16	0.07	0.01	0.00	92.41
A16-1	0.08	8.49	5.36	38.23	0.34	9.62	0.07	0.03	0.01	37.93	0.21	0.00	0.01	100.37
A16-2	0.06	7.96	4.91	40.39	0.44	8.58	0.21	0.02	0.02	36.81	0.15	0.00	0.01	99.58
A7-1	0.01	49.38	0.35	36.16	0.33	9.60	0.27	0.01	0.00	4.75	0.05	0.00	0.00	100.92
A9-2	0.03	51.14	0.19	41.00	0.60	7.63	0.22	0.04	0.00	0.09	0.03	0.01	0.00	100.99
A13-2	0.00	51.52	0.11	39.07	0.35	8.88	0.02	0.00	0.00	0.26	0.00	0.00	0.00	100.22
A14-1	0.02	49.95	0.40	35.42	0.29	9.95	0.05	0.02	0.00	4.35	0.06	0.00	0.00	100.52
A16-3	56.50	0.41	0.09	11.85	0.05	17.28	0.98	8.94	0.66	0.03	0.04	0.01	1.01	97.84
A5-2	0.00	0.02	0.01	8.81	0.82	12.30	32.19	0.05	0.01	0.02	0.07	0.02	0.01	54.32
A11-2	8.61	0.01	0.75	2.23	0.22	4.15	44.70	0.04	0.03	0.02	0.08	0.02	0.11	60.96
A14-2	0.58	0.02	0.01	6.15	0.22	20.35	33.27	0.09	0.06	0.01	0.05	0.00	0.11	60.92
A21-2	0.00	0.00	0.02	0.19	0.05	0.10	57.68	0.00	0.02	0.03	0.00	0.00	0.00	58.10
A4-3	0.00	0.04	0.00	0.36	0.02	0.01	8.56	0.20	0.02	0.02	0.00	0.00	0.01	9.25

Table 1: Mineral compositions, electron microprobe analyses.

Grain	Position	Image	Mineral	Type
A1-1	C	132	CPX	Macrocryst
A1-1	R	132	CPX	Macrocryst
A3-1	C	135	CPX	Macrocryst
A3-1	NEAR C	135	CPX	Macrocryst
A3-1	R	135	CPX	Macrocryst
A4-1	C	136	CPX	Macrocryst
A4-1	R	136	CPX	Macrocryst
A9-1	C	142	CPX	Macrocryst
A14-3	C	148	CPX	Macrocryst
A17-2	C	156	CPX	Macrocryst
A18-1	C	157	CPX	Macrocryst
A21-2	C	160,161	CPX	Macrocryst
A2-1	C	134	PHL	Macrocryst
A2-1	R	134	PHL	Macrocryst
A2-2	C	133	PHL	Macrocryst
A2-2	C	133	PHL	Macrocryst
A2-2	C	133	PHL	Macrocryst
A4-2	C	136	PHL	Incl. in cpx
A6-1	C	NONE	PHL	Macrocryst
A6-1	R	NONE	PHL	Macrocryst
A8-1	C	141	PHL	Macrocryst
A10-1	C	143	PHL	Macrocryst
A14-4	C	148	PHL	Macrocryst, intergr. w/ cpx
A14-6	C	149,150	PHL	Macrocryst, intergr. w/ mt
A17-1	C	156	PHL	Macrocryst
A17-1	R	156	PHL	Macrocryst, intergr. w/ cpx
A19-1	C	158	PHL	Matrix
A23-1	C	162	PHL	Macrocryst
A23-1	R	162	PHL	Macrocryst
A25-1	C	163	PHL	Macrocryst
A3-2	C	135	OX	Incl. in cpx
A5-1	C	137	MT	Macrocryst
A5-1	R	137	MT	Macrocryst
A7-2	C	139,140	OX	Macrocryst, intergr. w/ altered ol
A11-1	C	144	OX	Incl. in altered ol
A12-1		NONE	OX	Matrix
A13-1	C	145	MT	Macrocryst
A13-1	R	145	MT	Macrocryst
A14-5	C	149,150	MT	Macrocryst, intergr. w/ phl
A15-1	1	151	MT	Macrocryst
A15-1	2	151	MT	Macrocryst
A15-2	C	152	MT	Macrocryst
A15-3	C	153	MT	Macrocryst
A21-1	C	160,161	MT	Macrocryst, intergr. w/ cpx
A20-1	R	159	OX	Matrix
A16-1	C	154,155	CHR	Incl. in altered ol
A16-2	C	154,155	CHR	Incl. in altered ol
A7-1	C	139,140	ILM	Macrocryst
A9-2	C	142	ILM	Incl. in cpx
A13-2	C	146	ILM	Macrocryst
A14-1	C	147	ILM	Macrocryst
A16-3	C	154	AMPH	Alteration
A5-2	C	138	CARB	Alteration
A11-2	C	144	CARB	Alteration
A14-2	C	147	CARB	Alteration
A21-2	R	160,161	CARB	Alteration
A4-3		136	?	Vein in cpx

Table 2: Identification of electron microprobe analyses. Positions are marked in Appendix 1, CPX: clinopyroxene, PHL: phlogopite, MT: magnetite, CHR: Cr-spinel, ILM: ilmenite, OX: oxide (close to titanomagnetite composition), AMPH: amphibole, CARB: carbonate.

Chemical composition

The chemical composition of three selected wholerock samples with a minimum of xenoliths are given in Table 3. The major element analyses are by X-ray fluorescence on glass discs, and the analytical method is described by Kystol & Larsen (1999).

Sample	409788.1	409788.2	409788.5
SiO ₂	21.025	22.754	21.755
TiO ₂	2.676	2.418	2.563
Al ₂ O ₃	3.800	4.006	3.887
Fe ₂ O ₃	6.381	5.522	6.288
FeO	4.790	5.150	4.550
MnO	0.249	0.240	0.240
MgO	14.097	13.662	13.304
CaO	19.436	19.383	20.217
Na ₂ O	0.860	1.190	0.680
K ₂ O	2.436	2.336	2.616
P ₂ O ₅	1.425	1.375	1.435
Volat.	21.233	20.603	20.846
Sum, maj.	98.408	98.639	98.381
Sc	22	20	19.5
V	221	217	198
Cr	477	398	411
Co	51	50	51
Ni	154	140	138
Cu	130	135	136
Zn	118	115	125
Ga	13.8	13.1	13.7
Rb	86	81	87
Sr	2970	3768	3028
Y	35	35	35
Zr	989	1322	1229
Nb	252	231	257
Ba	1168	1087	1112
La	279	251	260
Ce	520	469	499
Pr	49	44	48
Nd	172	153	167
Sm	26	24	26
Eu	7.01	6.51	7.08
Gd	29	26	28
Tb	2.41	2.19	2.29
Dy	10.1	9.62	9.70
Ho	1.38	1.33	1.35
Er	3.56	3.32	3.37
Tm	0.37	0.35	0.35
Yb	1.97	1.83	1.81
Lu	0.28	0.26	0.26
Hf	15.0	15.5	15.1
Ta	15.3	13.1	15.1
Pb	8.61	26	8.83
Th	15.6	17.4	16.9
U	5.33	4.38	4.71

Table 3: Wholerock geochemical compositions by XRF on glass discs, and ICP-MS on wholerock solutions. SiO₂ to Volat. are given in wt. %, Sc to U in ppm.

Trace element analyses are by ICP-MS on whole-rock solutions, where machine calibration was done relative to three synthetic REE standards, BHVO and GH (Govindaraju, 1994). BHVO, GH and a basalt from Disko in West Greenland (DISKO-1) were analysed as unknowns along with the samples, and linear regressions calculated on plots of reference values against measured values for each element gave R^2 better than 0.9900 for all elements except Zr (0.9308) and Gd (0.979). The value of R^2 for a perfect fit is 1.0000. Element concentrations in the samples were corrected using the calculated regressions.

The high volatile contents are mainly due to the high amount of carbonate and phlogopite. The high MgO contents suggest that olivine may have been present in the rock, as is also suggested by the electron microprobe analyses of alteration phases, and the high P_2O_5 may indicate the presence of apatite. High Sr values are probably due to the presence of Sr-bearing carbonates, and the high concentrations of REE may also be hosted in carbonates, apatite or other accessory phases.

Classification

The whole rock compositions are comparable to aillikite compositions given by Rock (1986, 1991). These are ultramafic lamprophyres, which is consistent with the absence of feldspar in the groundmass. Lamprophyres from the Qaqarssuk carbonatite complex have compositions similar to the drillcore rock, whereas West Greenland kimberlites have higher MgO/CaO and SiO₂/Al₂O₃ ratios (Fig. 1).

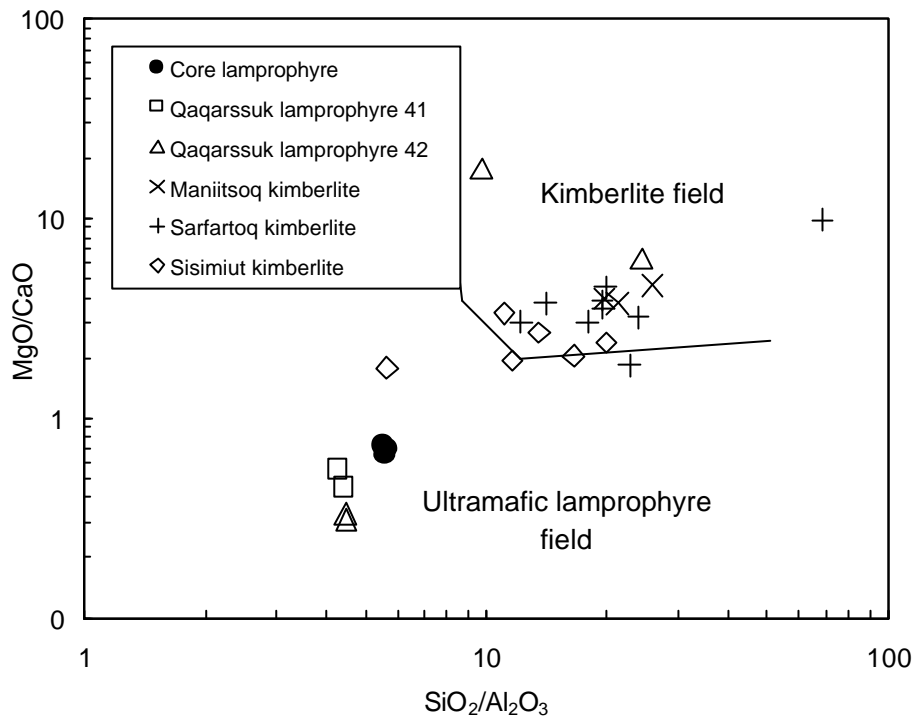


Fig. 1: Wholerock compositions of the drillcore lamprophyre compared with Qaqarssuk lamprophyres and kimberlites from the Maniitsoq, Sarfartoq and Sisimiut area. Qaqarssuk data are from Knudsen (1986), kimberlite data from Garrit (2000). Division lines are from Rock (1991).

Conclusions

The rock is phlogopite-ilmenite-magnetite-clinopyroxene macrocrystic with a groundmass consisting mainly of carbonate, titanomagnetite and phlogopite. Olivine is likely to have been present in the rock, but is now altered to mainly carbonates and some amphibole. It is best classified as an ultramafic lamprophyre, possibly an aillikite, and it has a composition similar to ultramafic lamprophyres from the Qaqarssuk complex.

References

Govindaraju; K. (1994): 1994 Compilation of working values and descriptions for 383 geo-standards. *Geostandards Newsletter* 118, 1-158.

Garrit, D. (2000): The nature of the Archaean and Proterozoic lithospheric mantle and lower crust in West Greenland illustrated by the geochemistry and petrography of xenoliths from kimberlites. Ph.D. thesis, University of Copenhagen.

Knudsen, C. 1986: Apatite mineralisation in carbonatite and ultramafic intrusions in Greenland. EEC contract MSM-119-DK. 176 pp + appendices.

Kystol, J. & Larsen, L.M. 1999: Analytical procedures in the Rock Geochemical Laboratory of the Geological Survey of Denmark and Greenland. *Geology of Greenland Survey Bulletin* 184, 59-62.

Rock, N.M.S. 1986: The nature and origin of ultramafic lamprophyres: alnöites and allied rocks. *Journal of Petrology* 27, 155-196.

Rock, N.M.S. 1991: *Lamprophyres*. Blackie & Son Ltd, 285 pp.

Secher, K. & Larsen, L.M. 1980: Geology and mineralogy of the Sarfartôq carbonatite complex, southern West Greenland. *Lithos* 13, 199-212.

Appendix 1

Electron backscatter images of minerals analysed with the electron microprobe.

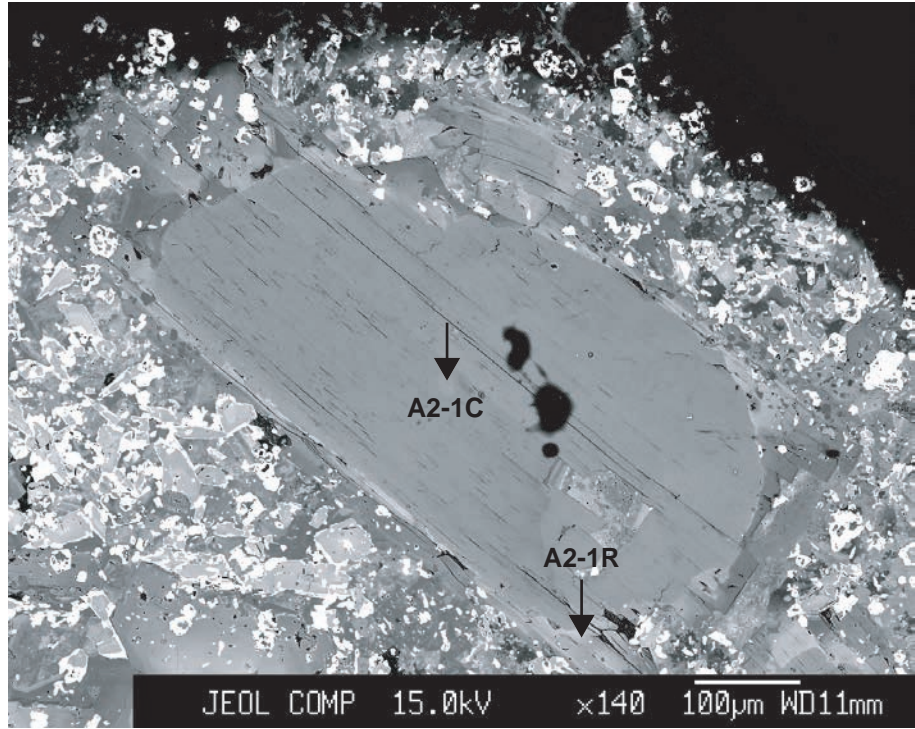


IMAGE 134: *Phlogopite macrocryst. Grain A2-1.*

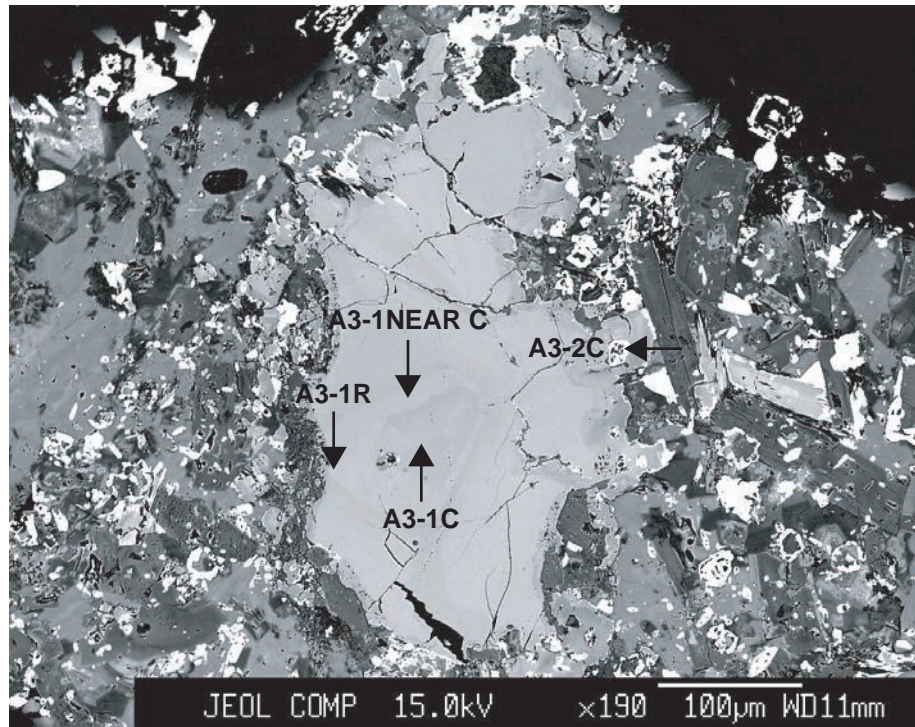


IMAGE 135: *Clinopyroxene macrocryst with oxide inclusion. Grains A3-1 and A3-2.*

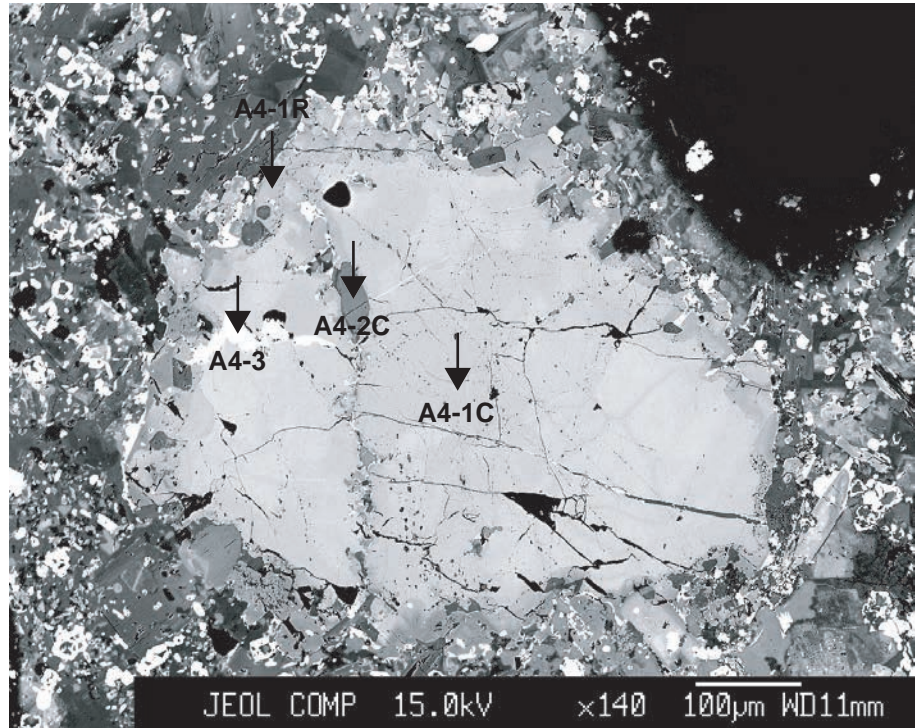


IMAGE 136: Clinopyroxene macrocryst with phlogopite inclusions and vein. Grains A4-1 and A4-2, vein A4-3.

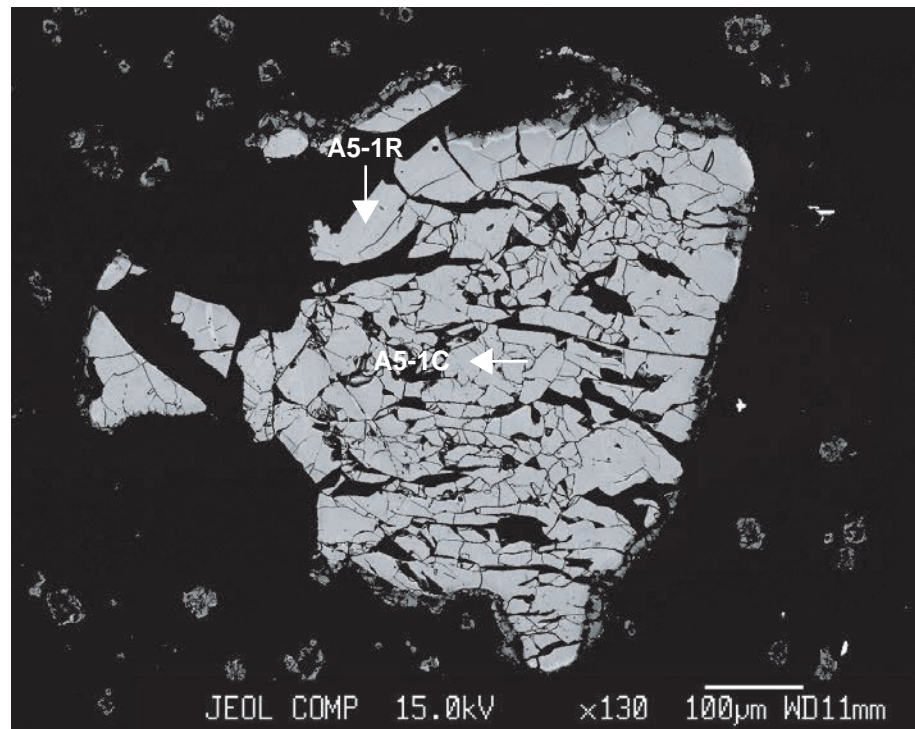


IMAGE 137: Magnetite macrocryst. Grain A5-1.

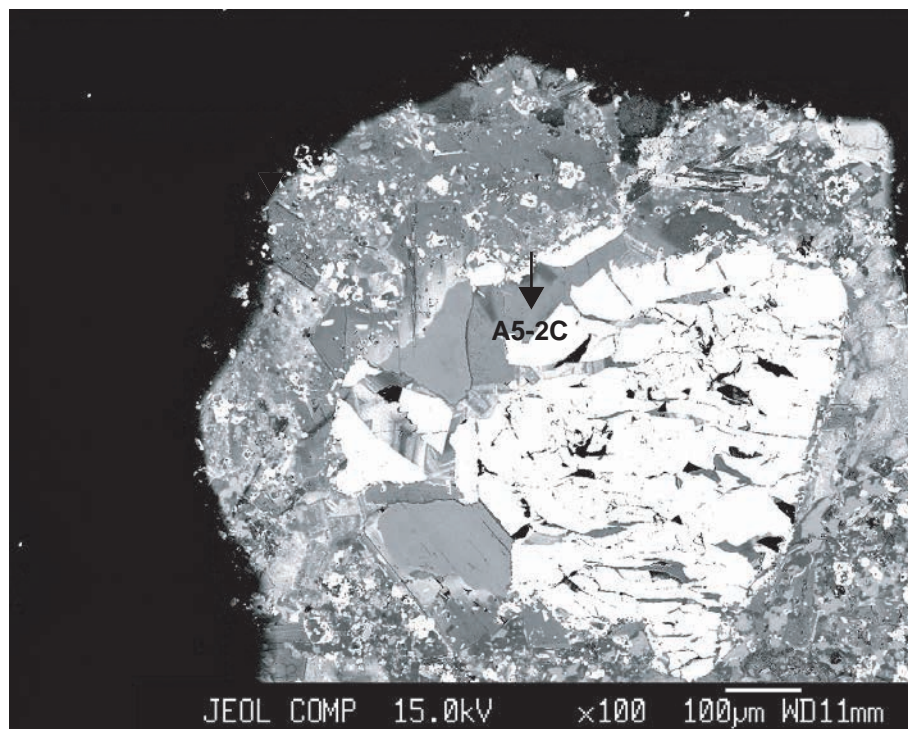


IMAGE 138: Magnetite macrocryst (see image 137) with alteration rim of phlogopite and carbonate (A5-2).

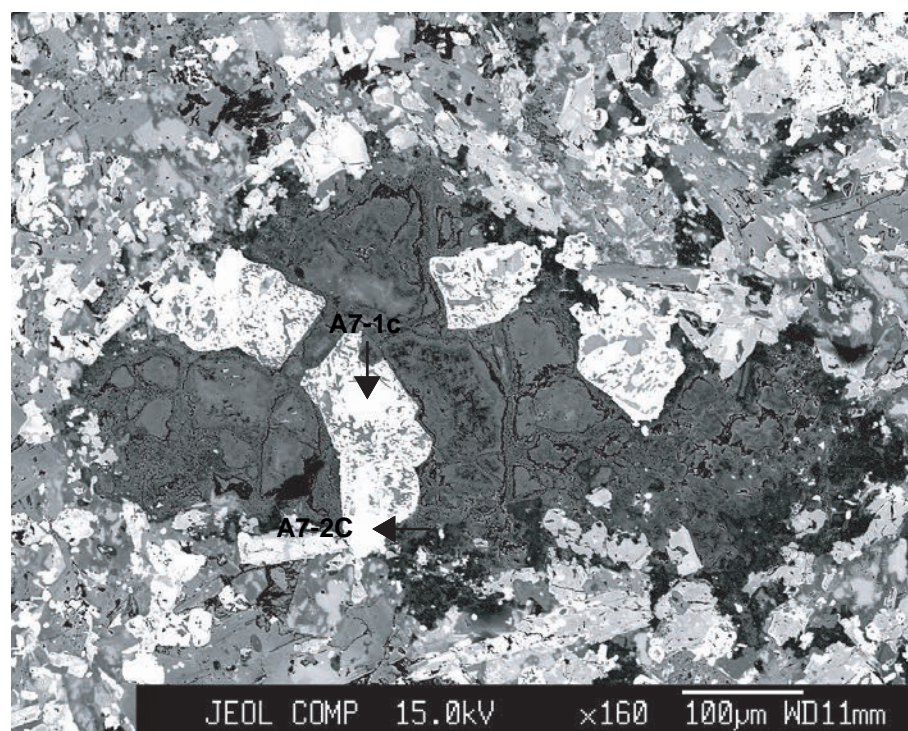


IMAGE 139: Oxide macrocrysts. Grains A7-1 and and A7-2 (see also image140).

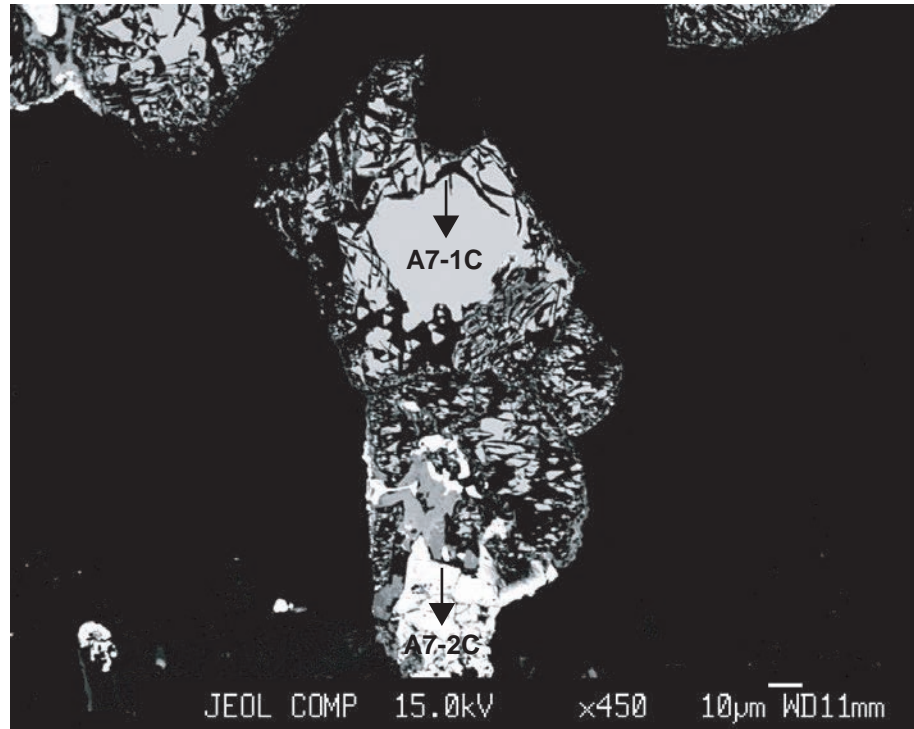


IMAGE 140: *Ilmenite macrocryst (A7-1) with alteration rim, and oxide (A7-2).*

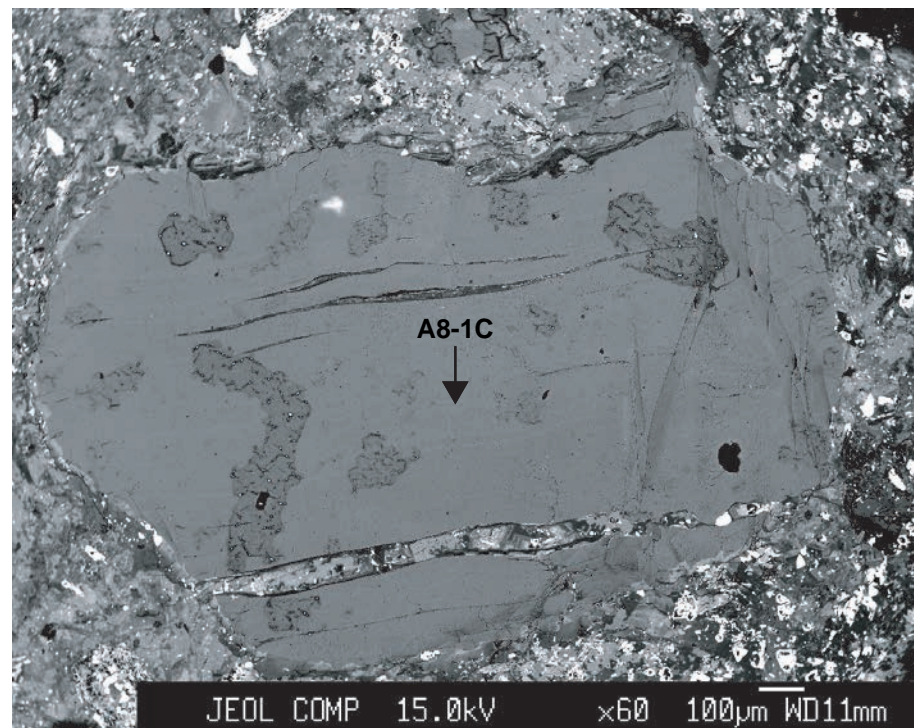


IMAGE 141: *Deformed phlogopite macrocryst. Grain A8-1.*

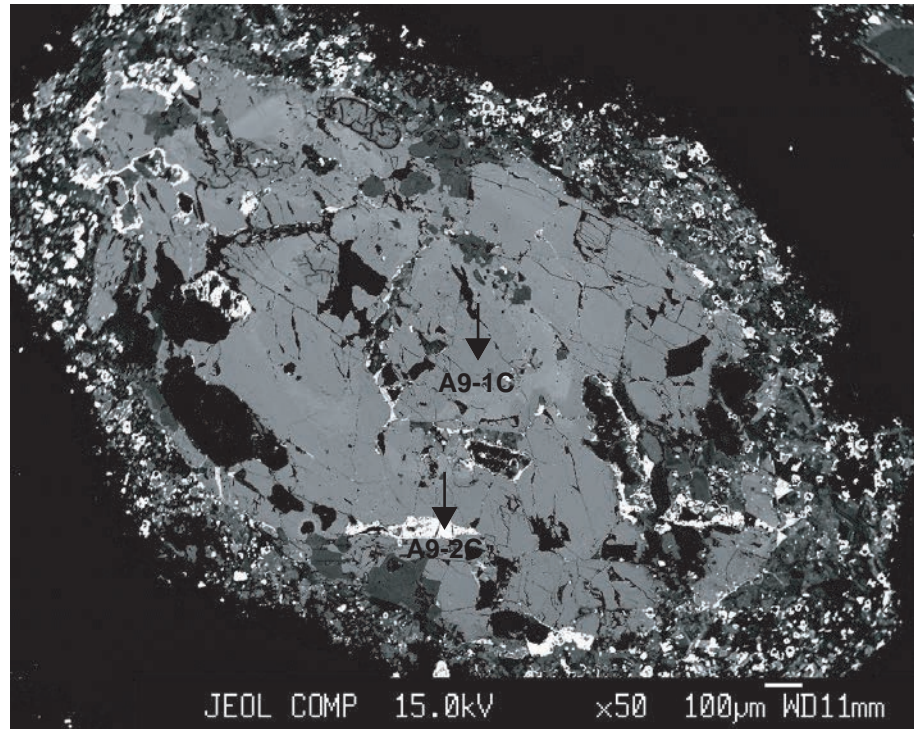


IMAGE 142: *Clinopyroxene macrocryst (A9-1) with ilmenite inclusion (A9-2).*

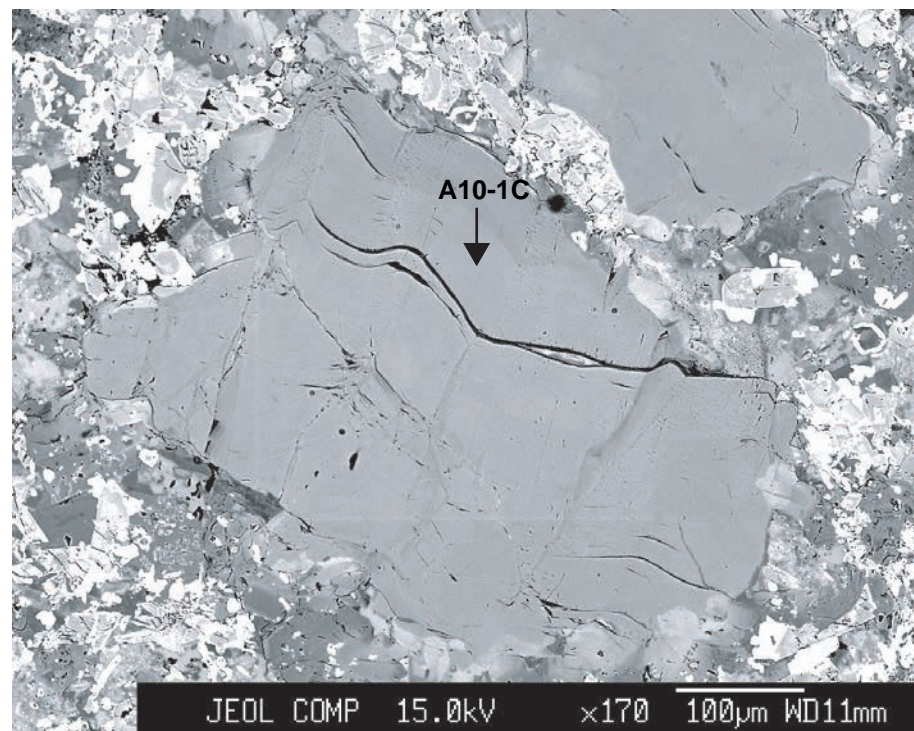


IMAGE 143: *Deformed phlogopite macrocryst. Grain A10-1.*

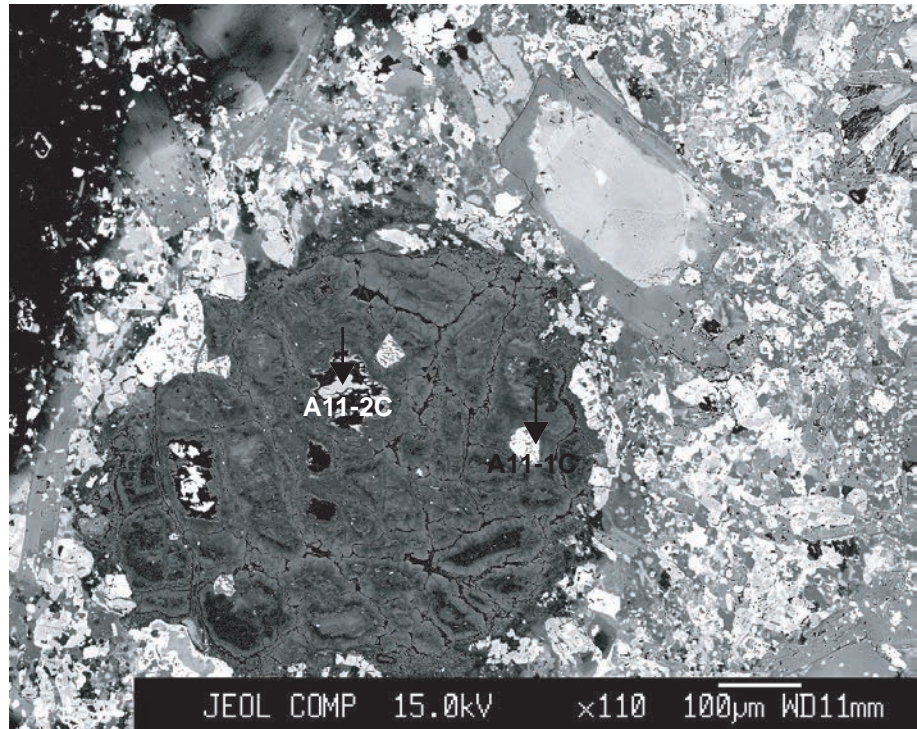


IMAGE 144: Altered olivine macrocryst with Cr-spinel inclusion (A11-1) and magnesianriebeckite (A11-2).

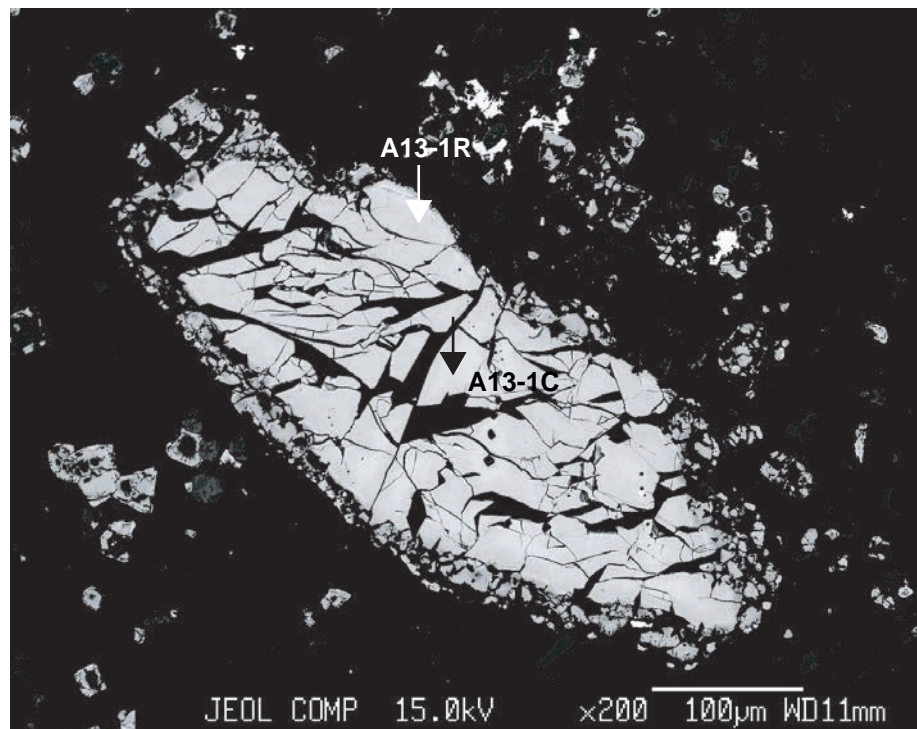


IMAGE 145: Magnetite macrocryst. Grain A13-1.

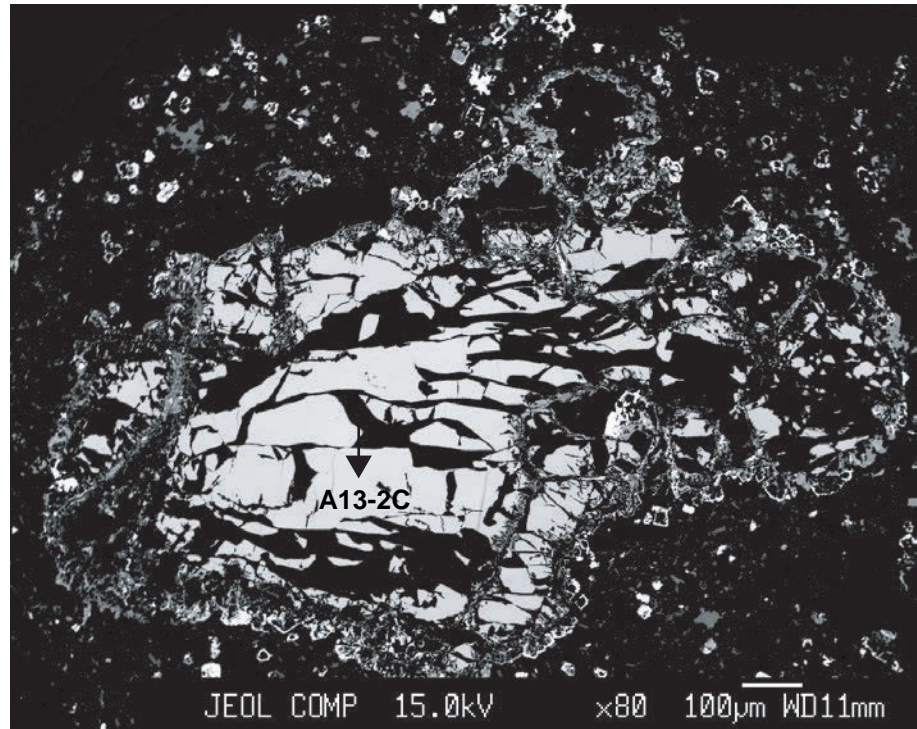


IMAGE 146: *Ilmenite macrocryst (A13-2).*

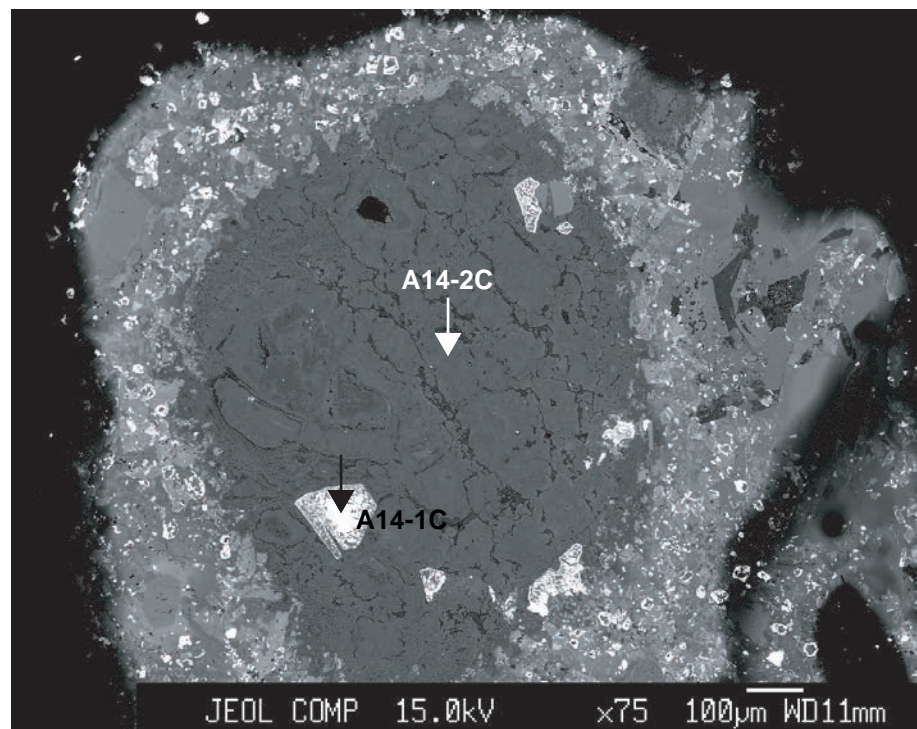


IMAGE 147: *Carbonate (alteration after olivine?, A14-2) and ilmenite inclusion (A14-1).*

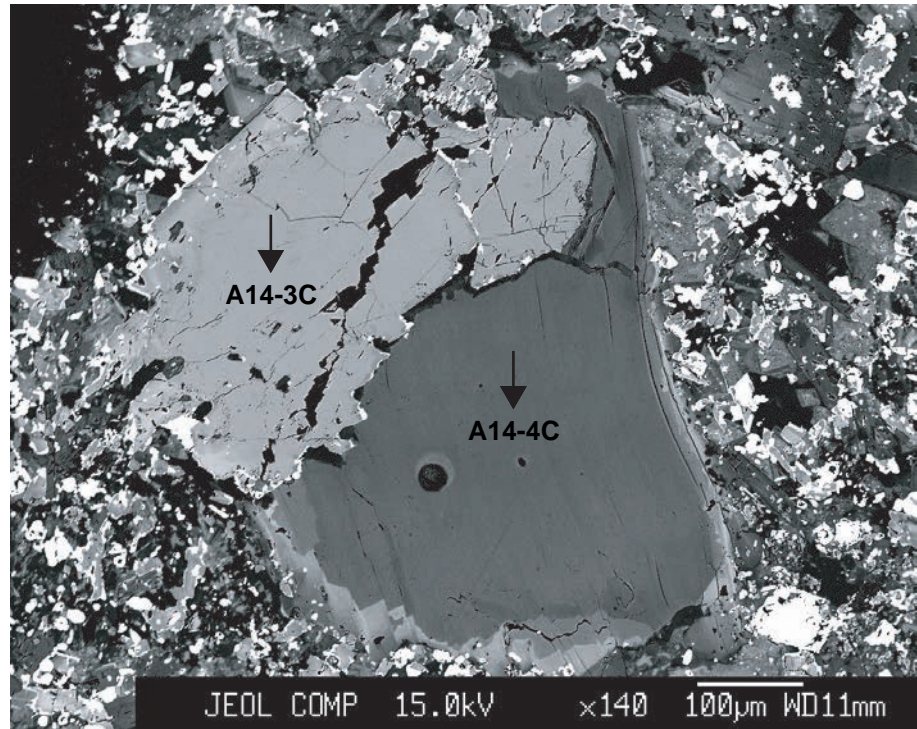


IMAGE 148: *Clinopyroxene macrocryst (A14-3) with phlogopite (A14-4).*

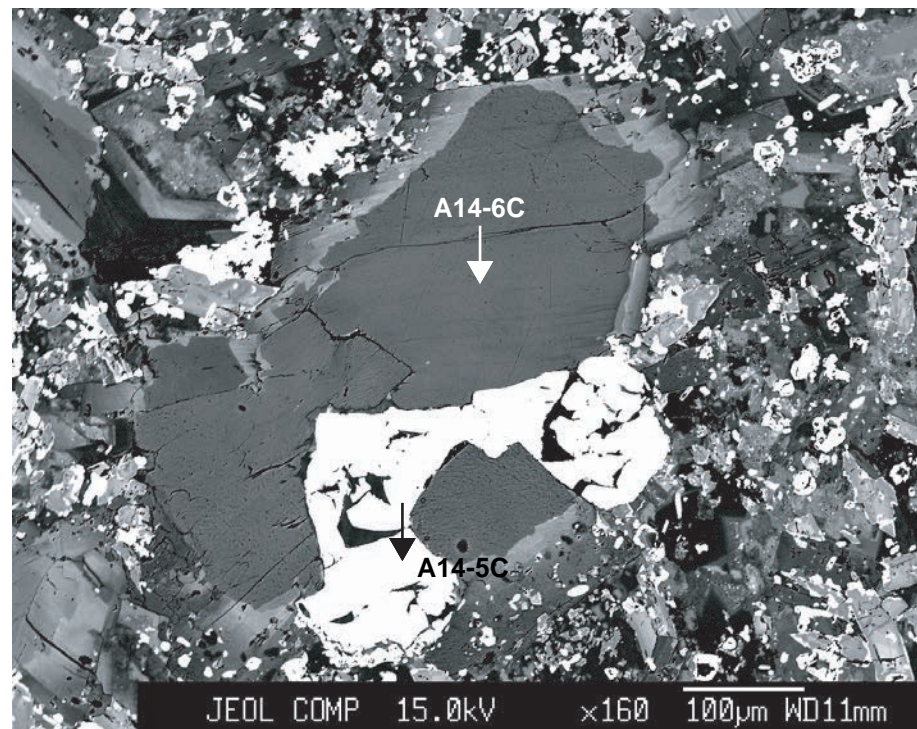


IMAGE 149: *Phlogopite (A14-6) and magnetite (A14-5) intergrowth.*

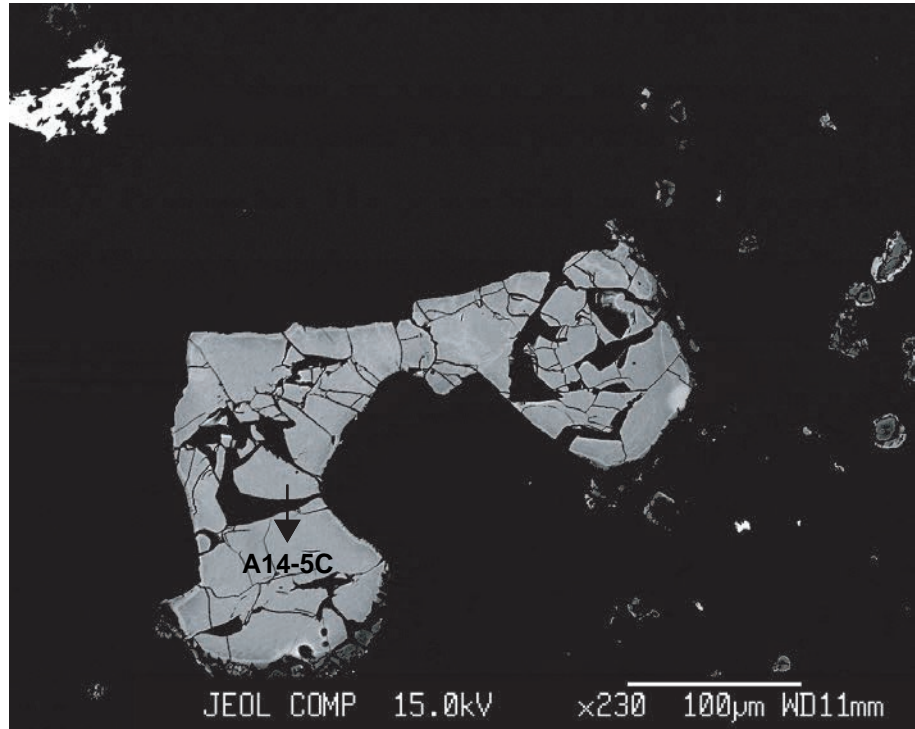


IMAGE 150: Same image as 149, enhanced for oxide compositional variations.

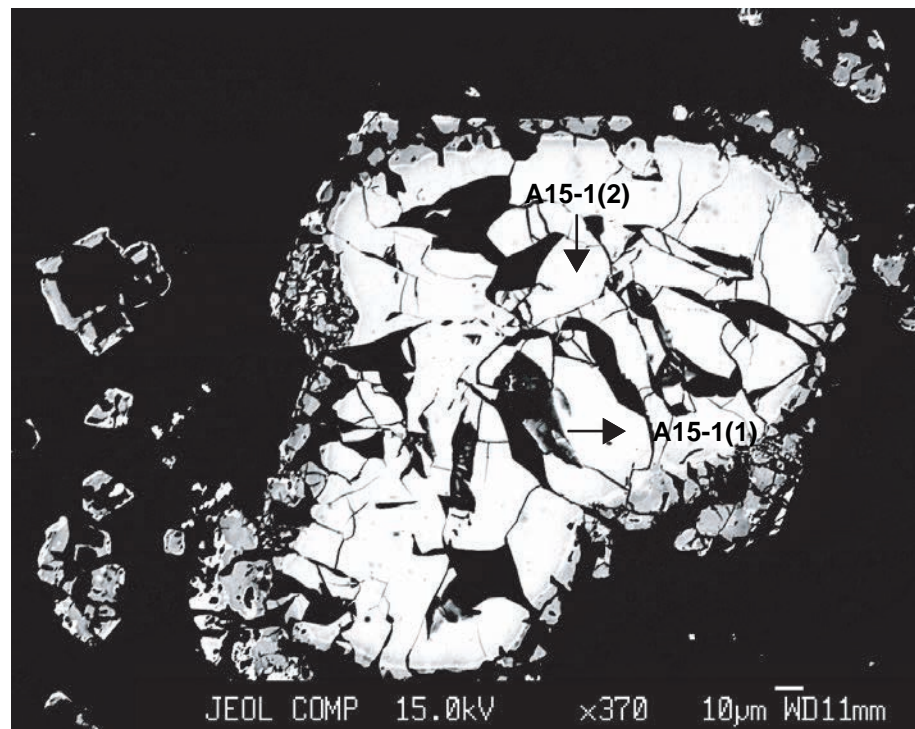


IMAGE 151: Magnetite macrocryst (A15-1).

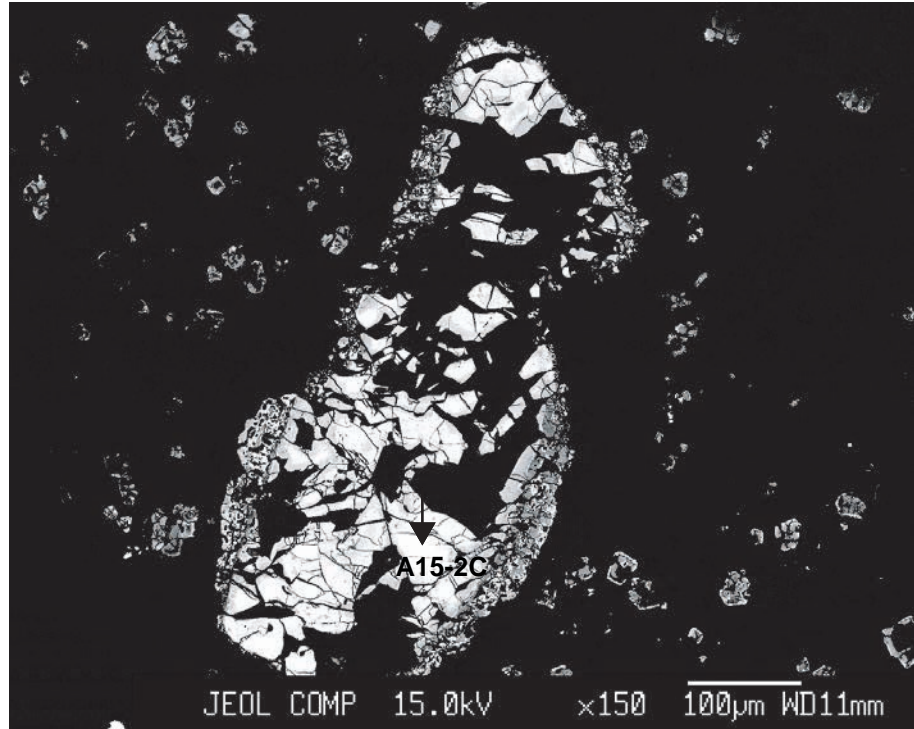


IMAGE 152: *Magnetite macrocryst (A15-2).*

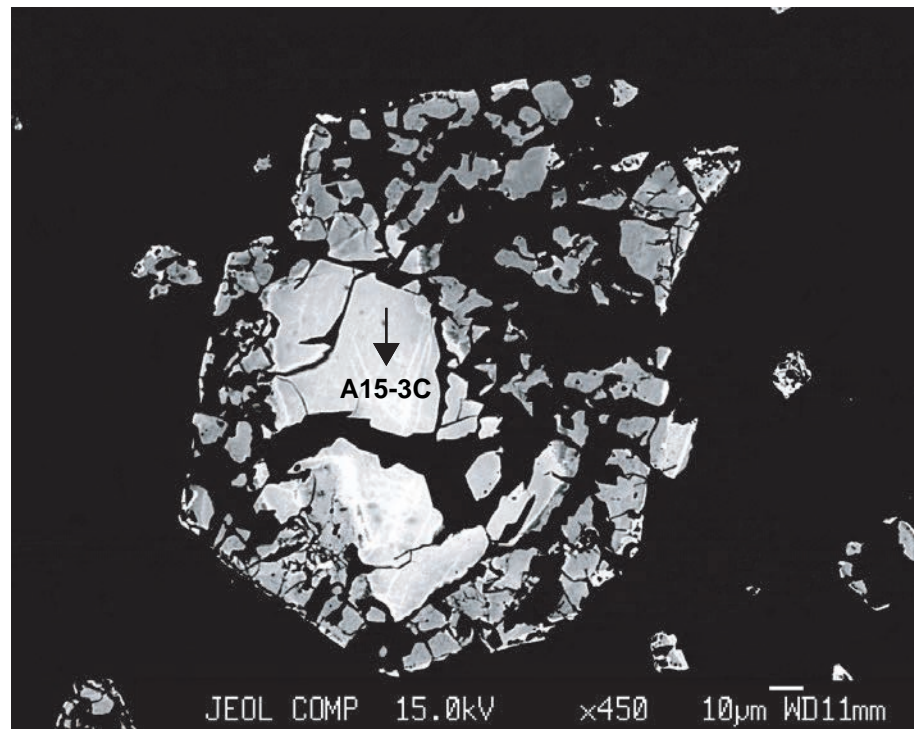


IMAGE 153: *Magnetite macrocryst (A15-3).*

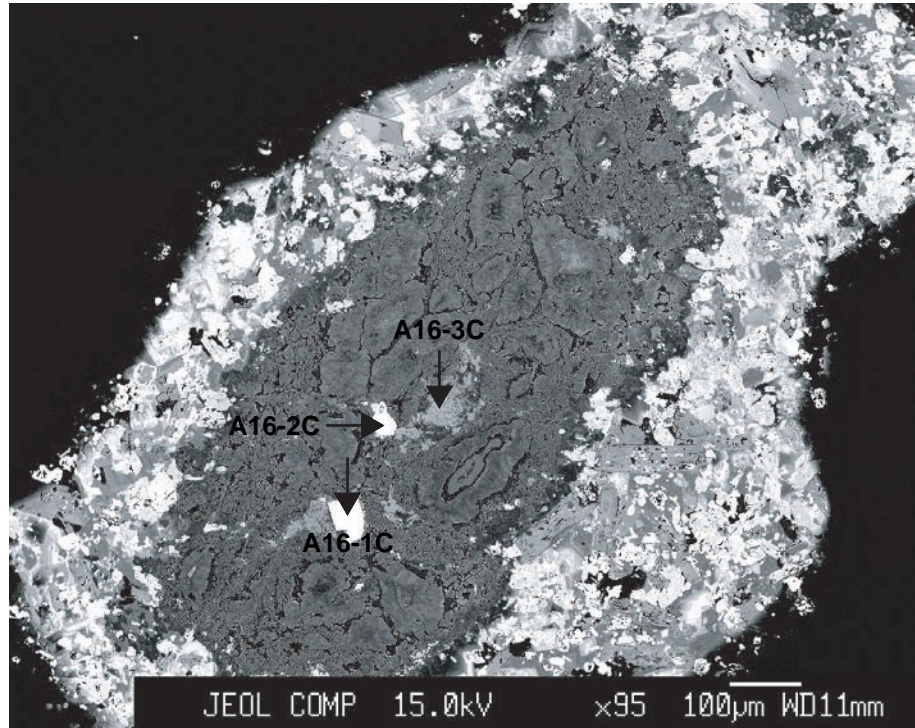


IMAGE 154: Altered olivine macrocryst with Cr-spinel inclusions (A16-1 & 2) and magnesioriebeckite (A16-3).

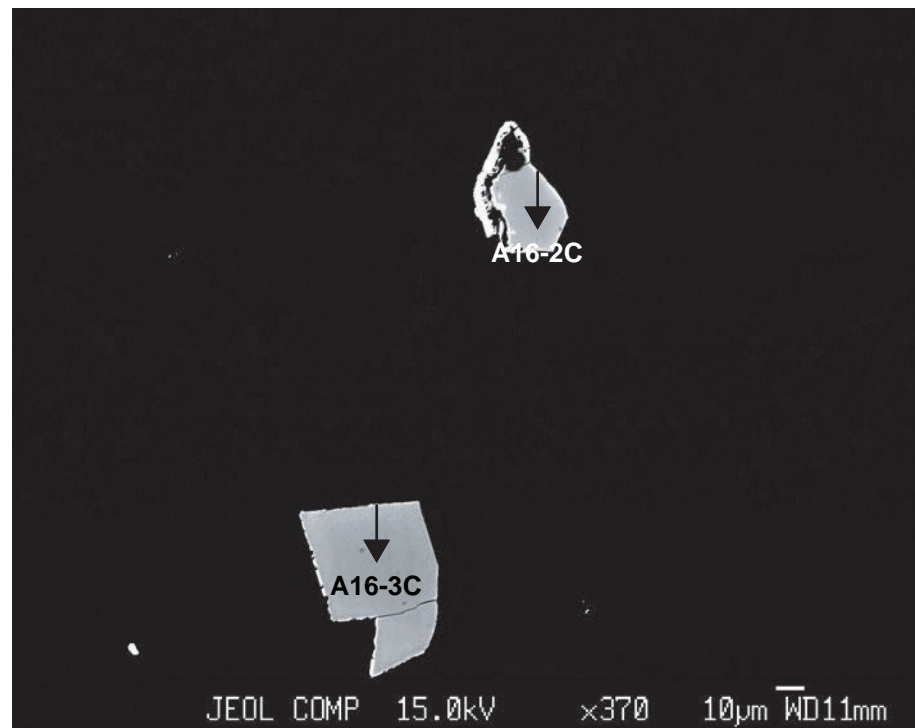


IMAGE 155: Cr-spinel inclusions in altered olivine (A16-1, A16-2).

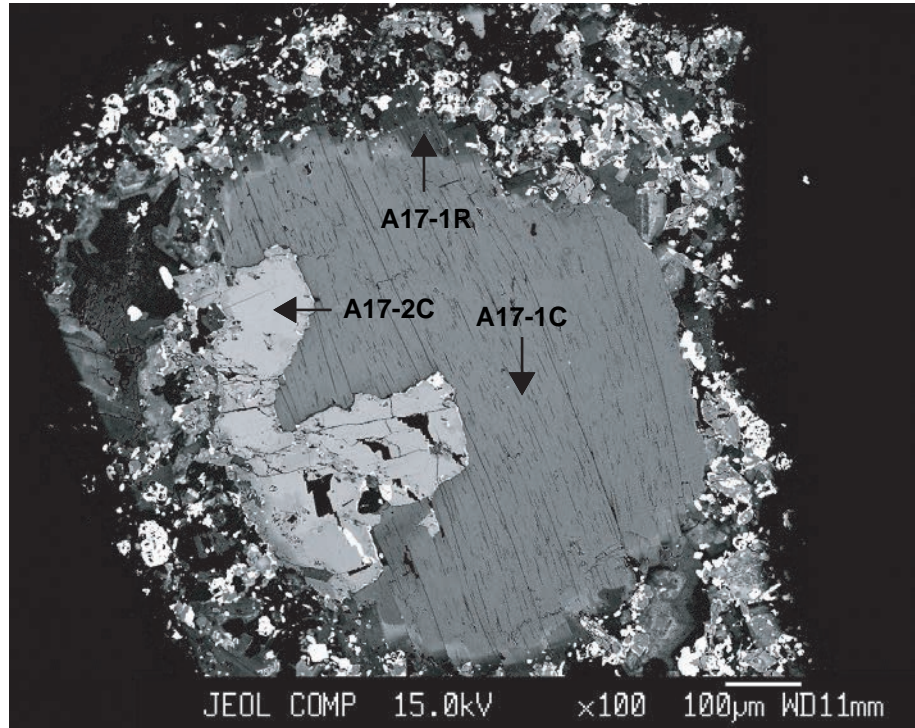


IMAGE 156: *Clinopyroxene (A17-2) and phlogopite (A17-1).*

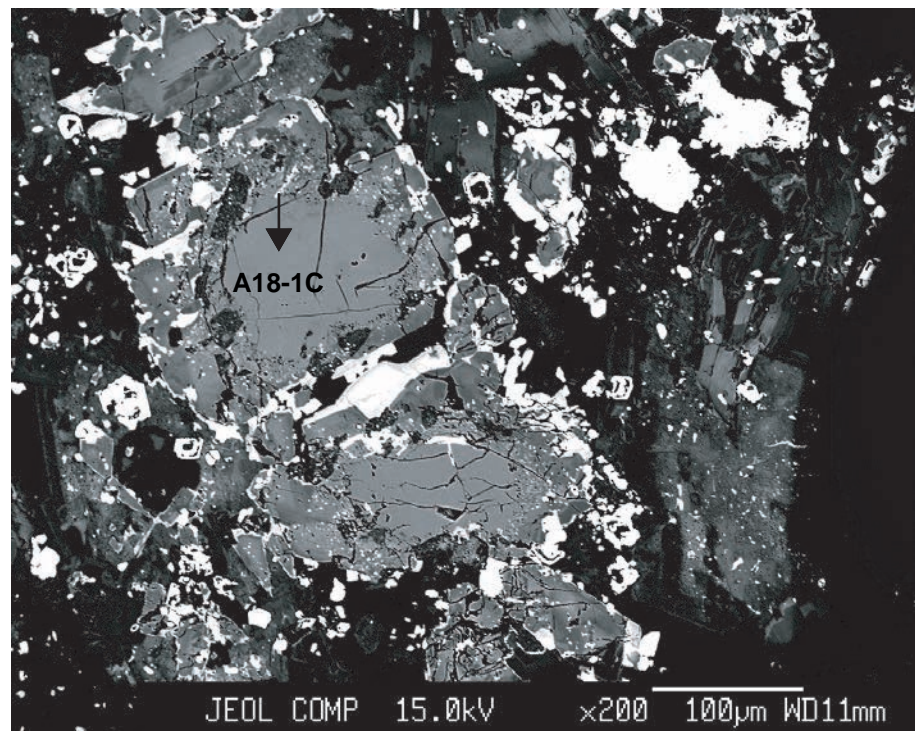


IMAGE 157: *Clinopyroxene macrocryst (A18-1).*

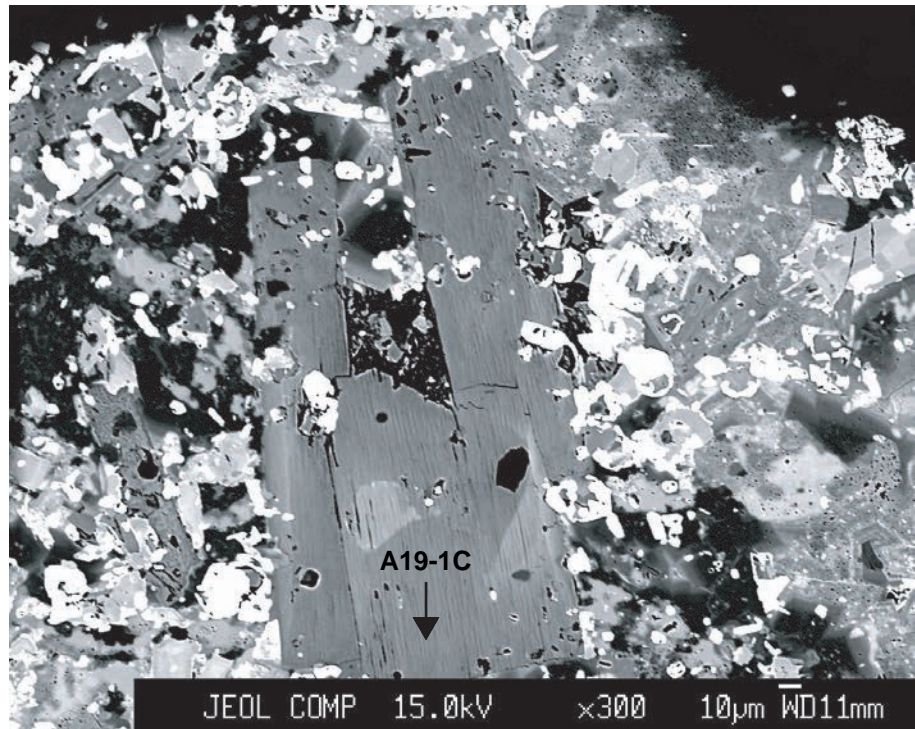


IMAGE 158: *Matrix phlogopite (A19-1).*

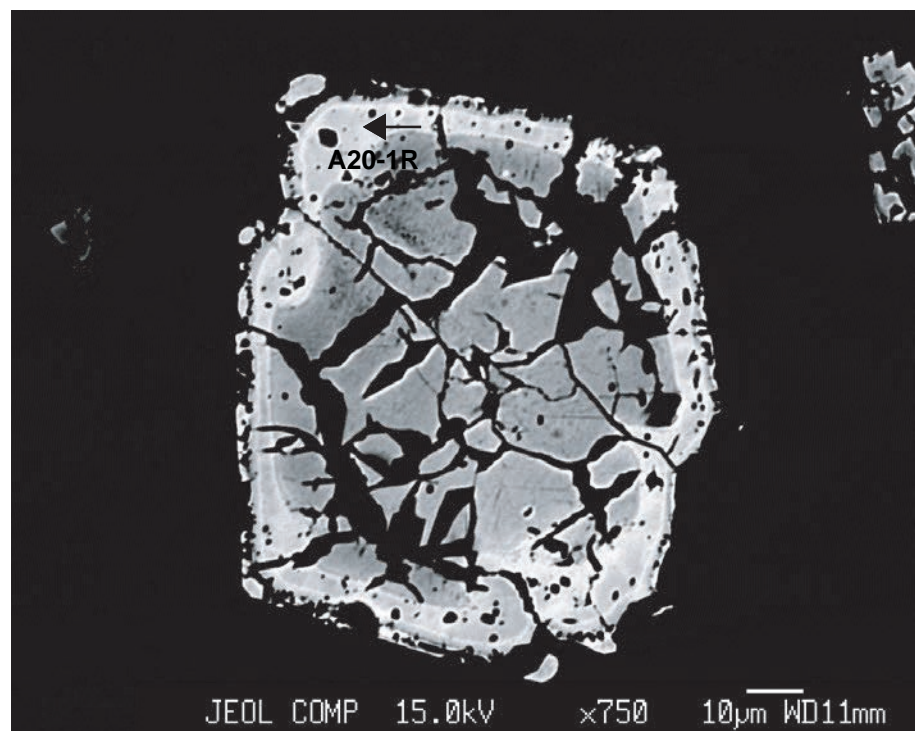


IMAGE 159: *Matrix oxide (A20-1).*

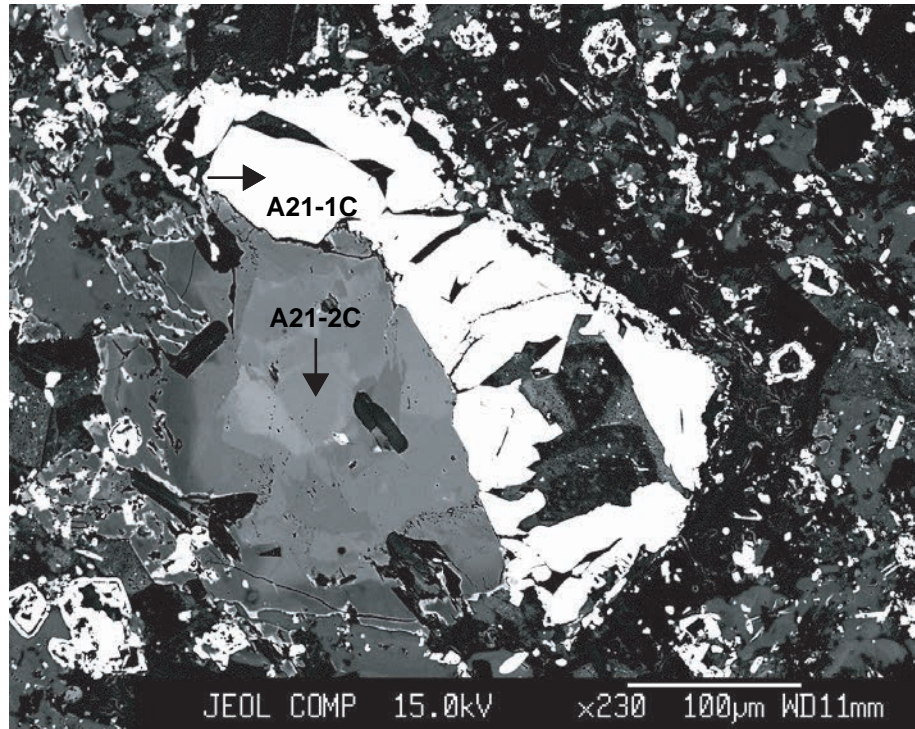


IMAGE 160: *Clinopyroxene (A21-2) and oxide (A21-1) intergrowth.*

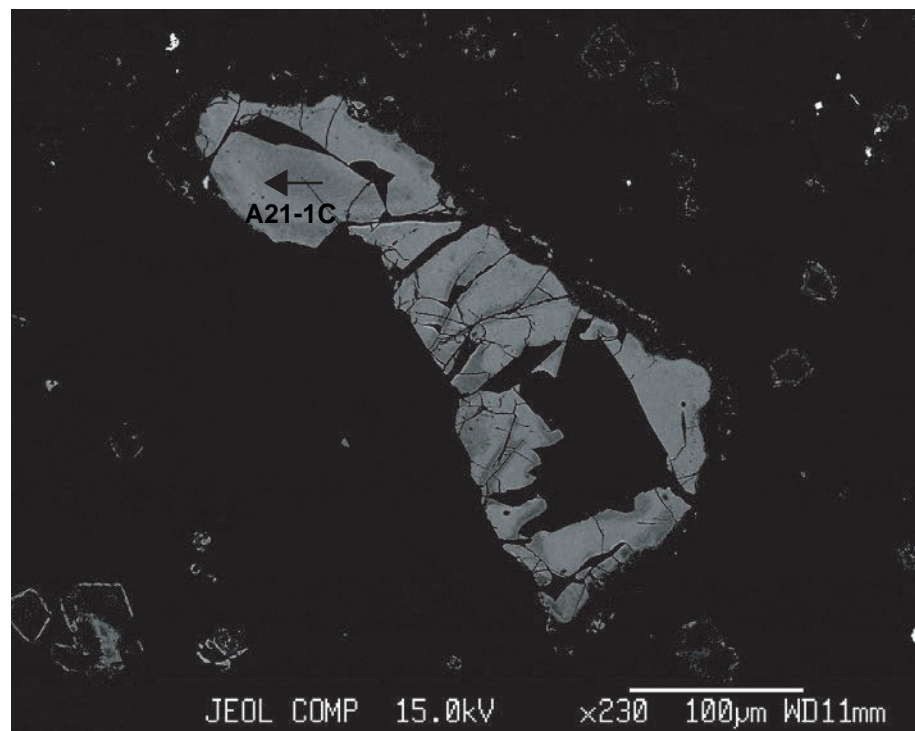


IMAGE 161: *Same as 160, enhanced for oxide compositional variations.*

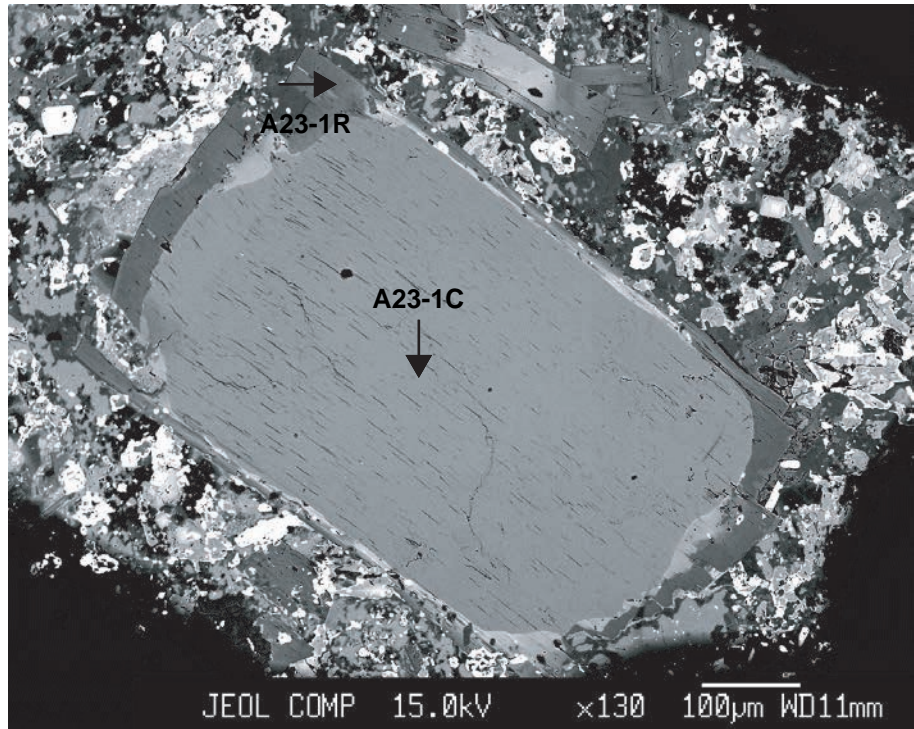


IMAGE 162: *Phlogopite macrocryst (A23-1).*

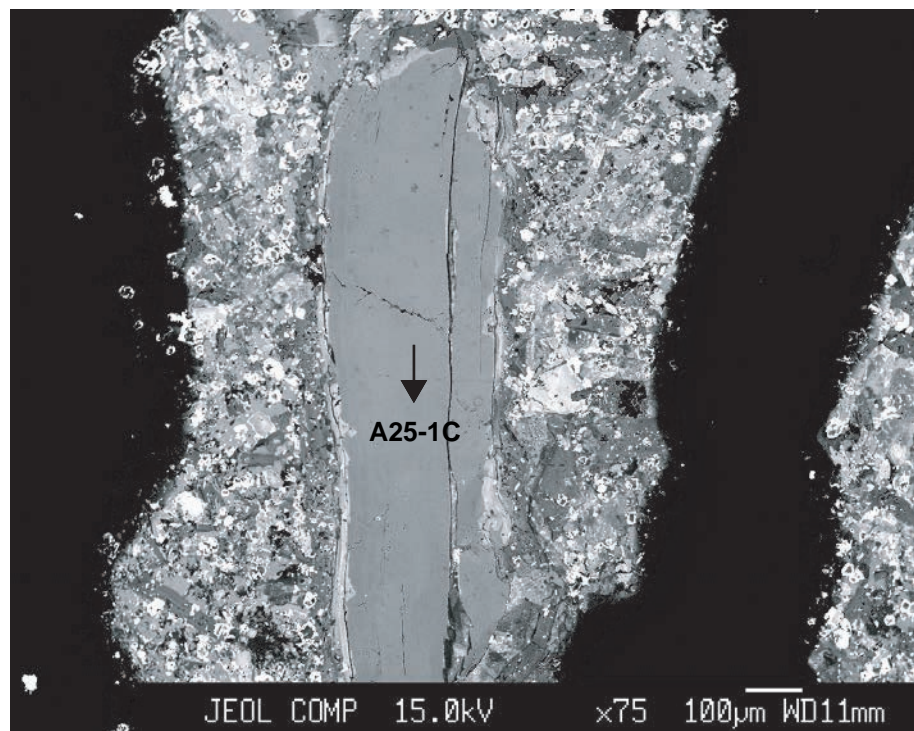


IMAGE 163: *Phlogopite macrocryst (A25-1).*